A Time Series Model of Interest Rates With the Effective Lower Bound*

Benjamin K. Johannsen†
Federal Reserve Board

Elmar Mertens
Federal Reserve Board

May 8, 2016

Abstract

Modeling interest rates over samples that include the Great Recession requires taking stock of the effective lower bound (ELB) on nominal interest rates. We propose a flexible time–series approach which includes a "shadow rate"—a notional rate that is less than the ELB during the period in which the bound is binding—without imposing no–arbitrage assumptions. The approach allows us to estimate the behavior of trend real rates as well as expected future interest rates in recent years.

*An earlier draft of this paper has been circulated under the title "The Shadow Rate of Interest, Macroeconomic Trends, and Time-Varying Uncertainty."

†For correspondence: Benjamin K. Johannsen, Board of Governors of the Federal Reserve System, Washington D.C. 20551. email benjamin.k.johannsen@frb.gov. Tel.: +(202) 530 6221. Future updates of this working paper can be downloaded from www.elmarmertens.com/research/workingpapers/JohannsenMertensShadowrate.pdf. We would like to thank seminar and conference participants at the 6th Joint BoC-ECB Conference — in particular our discussant Feunou Kamkui — the Federal Reserve Banks of Cleveland and Richmond, the Federal Reserve Board, the University of Texas at Austin, the World Congress of the Econometric Society (2015), and the Dynare Conference (2015), for their useful comments and suggestions. The views in this paper do not necessarily represent the views of the Federal Reserve Board, or any other person in the Federal Reserve System or the Federal Open Market Committee. Any errors or omissions should be regarded as solely those of the authors.

1 Introduction

This paper models nominal interest rates, along with other macroeconomic data, using a flexible time-series model that explicitly incorporates the effective lower bound (ELB) on nominal interest rates. We employ a modeling device that we refer to as a "shadow rate"—the nominal interest rate that would prevail in the absence of the ELB—which is conceptually similar to the shadow rates studied in the dynamic term–structure literature, as in Kim and Singleton (2011), Krippner (2013), Priebsch (2013), Ichiue and Ueno (2013), Bauer and Rudebusch (2014), Krippner (2015), and Wu and Xia (2016). Our time–series approach allows us to estimate the relationship between interest rates and macroeconomic data in a flexible way and, similar to the approach taken in Diebold and Li (2006), does not impose rigid no–arbitrage restrictions across the term–structure of interest rates.

We use our approach to estimate a trend–cycle model of U.S. data on interest rates, unemployment, and inflation over a sample that includes the recent spell at the ELB. Since the global financial crisis of 2008, real interest rates have been historically low, prompting some — for example, Summers (2014) and Rachel and Smith (2015) — to argue that the long–run normal level of real interest has fallen. Using our estimated model, we find that the trend component of the nominal interest rate has declined almost continuously since the early 1980s. The decline is due to long–standing downward trajectories of the trend component of both inflation and the real short–term interest rate. While uncertainty bands around our estimate of the trend real rate are wide, we find that any decline since the global financial crisis of 2008 is best characterized as a continuation of a longer term downward trajectory. Similar to Laubach and Williams (2003, 2015), Clark and Kozicki (2005), Hamilton et al. (2015), Kiley (2015), and Lubik and Matthes (2015) we find large uncertainty bands notwithstanding some differences in point estimates.[1] However, none of these papers explicitly models the ELB.

When we ignore the constraints imposed by the ELB on the data and proceed by applying a standard linear–state–space version of our model, we estimate a larger decline in the trend interest rates in recent years than in our model with the ELB. The reason is that the gap be-

[1]Notably, our estimated trend real rate displays less movement than the trend estimates reported by Laubach and Williams (2003, 2015), and does not not dip as low during the recent recession.

tween the observed interest rates and the estimated trend is not as large as the gap between our estimated shadow rate and the trend. Without a large cyclical movement associated with the Great Recession, the model has an easier time explaining the prolonged period with the short–term interest rate at the ELB as a change in trend. Additionally, explicitly modeling the ELB has large effects on inference about out–of–sample expected short–term interest rates and term premiums over the past several years. Our estimated shadow rates are less than the ELB by construction, and our shadow–rate model delivers predicted paths for future short–term interest rates that include extended periods at the ELB. By contrast, when we ignore the ELB, the model predicts relatively precipitous increases in short–term rates.

We find that including a medium–term interest rate in our model—which is not constrained by the ELB over our data sample—disciplines the behavior of the shadow rate, reflecting the model's estimated co–movement between yields of different maturity. Without the medium–term yield, our shadow rate estimates would merely reflect the dynamic relationship between short–term interest rates and the macroeconomic variables in our data set (unemployment and inflation). However, inasmuch as medium-term rates contain useful information about the path of expected future short–term rates, the medium-term interest rate helps us identify and forecast the shadow rate above and beyond the information gleaned from the macroeconomic data in our sample.

The way we incorporate the ELB and estimate the model can be extended to a broad class of time series models. With short–term nominal interest rates at or near their ELBs in many parts of the world, time series models that include interest rates but ignore the ELB—like a standard vector autoregression—have been unable to adequately address the data. Moreover, reduced-form explorations of the empirical relationship between short– and longer–term interest rates—such as Campbell and Shiller (1991)—have often ignored the truncation in the distribution of future short–term interest rates. Our modeling approach overcomes these shortcomings in a wide class of otherwise conditionally–linear Gaussian state–space models. Examples include the vector autoregressions studied in Sims (1980) and the models with time–varying parameters studied in Primiceri (2005) and Cogley and Sargent (2005b).

Following work by Black (1995), the no–arbitrage dynamic term–structure models stud-

ied in Kim and Singleton (2011), Krippner (2013), Priebsch (2013), Ichiue and Ueno (2013), Bauer and Rudebusch (2014), Krippner (2015), and Wu and Xia (2016) identify shadow rates by imposing no–arbitrage cross–equation restrictions. These studies offer interesting insights, yet the no–arbitrage assumptions that these authors maintain may preclude certain model features, like stochastic model parameters. Our time series approach naturally incorporates time variation in parameters, and thus, for some purposes—like including time–varying trends in inflation and interest rate data or modeling stochastic volatility—offers a flexible alternative. In addition, our shadow–rate estimates do not only reflect information embedded in longer–term yield data but also condition on direct readings about business cycle conditions embedded in macro variables such as the unemployment–rate gap and inflation.[2]

Iwata and Wu (2006), Nakajima (2011), Chan and Strachan (2014) are the closest papers in the literature to ours. These papers also estimate time series models that incorporate the ELB. In all of these studies, lagged observed interest rates (rather than shadow rates) are explanatory variables in the dynamic system. We instead allow lagged shadow rates to be explanatory variables. In doing so we are able to more closely align our approach with the no–arbitrage term–structure literature, and, in additional, connect the concept of the shadow rate with the level of the short–term rate that would prevail in the absence of the ELB because we allow it to have the same persistence and co–variance properties as short–term interest rates. Nevertheless, our approach is flexible enough to include both shadow rates and observed rates as lagged explanatory variables.

2 A Model of Interest Rates and the ELB

In this section we describe our time–series model, which explicitly includes the ELB. The model includes inflation, a short– and a medium–term nominal interest rate, and the

[2]In an alternative time-series approach Lombardi and Zhu (2014) use a dynamic factor model to derive estimates of the stance of monetary policy — labeled "shadow rate" — from interest rates, monetary aggregates and variables characterizing the Federal Reserve's balance sheet. However, as such, their underlying shadow–rate concept is quite different from what is used here or in the dynamic term-structure literature in that their measure needs not be identical to observed interest rates, even when the ELB is not binding, nor is their shadow rate constrained to lie below the ELB when the bound is binding.

unemployment–rate gap as measured by the CBO.

2.1 The Shadow Rate Approach

Our data set includes a short–term interest rate, which has been at the ELB during 28 quarters in our sample. We model the interest rate (i_t) as the observation of a censored variable. In particular, we assume that the nominal interest rate is the maximum of the ELB and a shadow rate (s_t) so that

$$i_t = \max\left(s_t, ELB\right) \ . \tag{1}$$

The ELB might arise because of an arbitrage between bonds and cash, though the world has seen negative short–term nominal interest rates in a number of countries. It also might be thought of as a level below which monetary authorities are unwilling to push short–term interest rates. For our purposes, it is taken as an exogenous known constant (which could be made time–varying). We proceed by modeling the shadow rate, in conjunction with the other variables in the model, using standard time–series methods, and account for the ELB when conditioning the posterior distribution of our model on observed interest rate data.

2.2 A Time Series Model with Shadow Rates

We assume that inflation (π_t), the medium–term yield (y_t), and the shadow rate (s_t) can be decomposed into trend and cyclical components. That is, for every data series, x_t, we assume that

$$x_t = \bar{x}_t + \tilde{x}_t \qquad \text{where} \quad \bar{x}_t = \lim_{h\to\infty} E_t\left(x_{t+h}\right) \qquad \text{and} \quad E(\tilde{x}_t) = 0 \tag{2}$$

The defining feature of the cyclical (gap) component, $\tilde{x}_t$, is that it has a zero ergodic mean. For the unemployment rate (u_t) we assume that the gap measure derived from subtracting the CBO's measure of the long-run natural rate from the actual unemployment rate reflects a detrended series akin to the $\tilde{x}_t$ component in (2).

The trend components $\bar{x}_t$ are similar in spirit to the trend concept of Beveridge and Nelson (1981); however, by treating the trends as unobserved components we allow for the conditional expectations, $E_t(\cdot)$ in (2), to reflect a possibly wider information set than what is known to an econometrician at time t.[3] Defining the trend components as infinite-horizon expectations implies that changes in $\bar{x}_t$ follow martingale-difference processes; and, as a result, the trend components have unit root dynamics. As documented, for example, by Stock and Watson (2007) and Cogley and Sargent (Forthcoming), U.S. inflation dynamics are well captured by such a trend-cycle decomposition when trend shocks have time-varying volatility. So, for the trend component of inflation, we write:

$$\bar{\pi}_t = \bar{\pi}_{t-1} + \sigma_{\bar{\pi},t}\epsilon_{\bar{\pi},t}. \tag{3}$$

where $\epsilon_{\bar{\pi},t} \sim N(0,1)$. (Throughout the text $\epsilon_{\cdot,t}$ and $\eta_{\cdot,t}$ indicate uncorrelated standard–normal random variables.)

Away from the ELB, our shadow rate is identical to the short–term nominal interest rate. We assume that the trend shadow rate has two components

$$\bar{s}_t = \bar{\pi}_t + \bar{r}_t \tag{4}$$

where $\bar{r}_t$ will be our measure of the trend in real interest rates, discussed below. We assume that $\bar{r}_t$ evolves so that

$$\bar{r}_t = \bar{r}_{t-1} + \sigma_{\bar{r}}\epsilon_{\bar{r},t}. \tag{5}$$

To capture a connection between short– and medium–term interest rates, we assume that the medium–term rate in our model (y_t) shares a common trend with the shadow rate, adjusted for an average term–premium.[4] By assuming that yield spreads are stationary, we impose the

[3] See also the discussion in Mertens (forthcoming).

[4] Specifically, the trend in the nominal medium-term yield is written as $\bar{y}_t = \bar{s}_t + \bar{p}_0$ where the constant $\bar{p}_0$ represents the average term–premium, and its estimated value reflects the average spread between medium- and short–term nominal interest rates in our sample (away from the ELB). As for all gap variables, the mean of the medium-term yield gap, $E(\tilde{y}_t)$, has been normalized to zero. In principle, the distinction between shadow rates and observed nominal

same cointegrating relationship on nominal yields that has also been used by Campbell and Shiller (1987) and King and Kurmann (2002). In sum, there are two stochastic trends in our model: $\bar{\pi}_t$ and $\bar{r}_t$.

Prior evidence suggests that shocks to trend inflation have been most likely highly heteroscedastic (Stock and Watson, 2007) in U.S. postwar data, possibly reflecting changes in the anchoring of public perceptions of long–term inflation expectations and the credibility of policymaker's inflation goals. By contrast, the variability of the trend real rate is more likely to reflect changes in long–term growth expectations, demographic trends and other secular drivers (Rachel and Smith, 2015) and accounts probably only for a small share of the variability in real rates as discussed, for example, by Hamilton et al. (2015), which cautions us against fitting a stochastic volatility process for changes in this trend. Accordingly, shocks to trend inflation are assumed to be affected by stochastic volatility in our model, whereas we have chosen to specify a constant variance for the shocks to $\bar{r}_t$; in addition, both trend shocks are supposed to be mutually uncorrelated.

We assume that the gap components of the four series in our model follow a joint autoregressive process. That is,

$$\boldsymbol{A}(L) \begin{bmatrix} \tilde{\pi}_t \\ \tilde{u}_t \\ \tilde{s}_t \\ \tilde{y}_t \end{bmatrix} = \boldsymbol{B}\boldsymbol{\Sigma}_t \boldsymbol{\epsilon}_t \tag{6}$$

where $\boldsymbol{A}(L)$ is a polynomial in the lag operator, which has roots outside the unit circle, $\boldsymbol{B}$ is a unit–lower–triangular matrix, and $\boldsymbol{\Sigma}_t$ is a diagonal matrix.

We include time–varying volatility in the shocks to the trend component of inflation and in the gap–vector autoregression. We assume that $\sigma^2_{\bar{\pi},t}$ and the diagonal elements of $\boldsymbol{\Sigma}_t$ follow a

rates could also be extended here to the nominal medium-term yield and its trend; however, in our application the distinction would be moot since the ELB never binds for the medium-term yield in our data.

process given by

$$\log\left(\sigma_{j,t}^2\right) - \mu_j = \rho_j\left(\log\left(\sigma_{j,t-1}^2\right) - \mu_j\right) + \phi_j\eta_{j,t} \tag{7}$$

where $\sigma_{j,t}^2$ denotes a particular diagonal element of $\mathbf{\Sigma}_t$ or $\sigma_{\bar{\pi},t}^2$, μ_j is the mean of the log of the variable j, ρ_j is the persistence of the process, and σ_j is the volatility of innovations. Stochastic volatility helps us capture the run up in average inflation in the late 1970s and early 1980s and gives the model flexibility to capture large changes in the gap components over the business cycle.

Finally, we assume that observed inflation is the sum of $\bar{\pi}_t$, $\tilde{\pi}_t$, and measurement error with stochastic volatility:

$$\pi_t = \bar{\pi}_t + \tilde{\pi}_t + e_t^{\pi}, \qquad\qquad e_t^{\pi} = \sigma_{e,t}\epsilon_{e,t} \tag{8}$$

The inclusion of measurement error helps us capture highly transitory, one–off movements in headline inflation that do not feed back into real activity.

2.3 Relationship Between Shadow and Interest Rates

We conceptualize the shadow rate as the nominal interest rate that would prevail in the absence of the ELB. On a period–by–period basis, the interest rate is either equal to the shadow rate or equal to the ELB. The key distinction between shadow rates and interest rates is thus that shadow rates have unbound support.

In the model we presented in the previous section, we modeled the shadow–rate gap, as well as its lags, as part of a joint dynamic system, which allows the shadow rate to have the same persistence properties when the ELB is binding and when it is not. By contrast, Iwata and Wu (2006) and Nakajima (2011) model the variables in their models as functions of lagged observed interest rates. This means that, in those papers, at the ELB the value of the shadow–rate in the previous period has no direct effect on its value today. This approach is in stark contrast to the shadow–rate dynamics from dynamic term–structure literature; see, for

example, Wu and Xia (2016).

Similar to the term-structure literature, we embed the shadow rate into a state vector with auto–regressive dynamics, such that the persistence of the shadow rate does not depend on whether the ELB binds. When the ELB is binding on observed interest rates, the shadow rate is intended to capture the hypothetical level of the nominal rate that would prevail in the absence of the ELB constraint; accordingly, we deem it beneficial that the estimated persistence of the shadow rate in our specification, reflects to a large degree the persistence of observed interest rates when those are away from the ELB.

2.4 Interpretation of $\bar{r}_t$

Because interest rates are truncated shadow rates, the expected interest rate is necessarily weakly larger than the expected shadow rate. In turn, it is also the case that,

$$\lim_{h\to\infty} E_t\left(i_{t+h}\right) \geq \lim_{h\to\infty} E_t\left(s_{t+h}\right) = \bar{s}_t = \bar{\pi}_t + \bar{r}_t. \tag{9}$$

In our model, $\bar{s}_t$ is the median forecast of $\lim_{h\to\infty} i_{t+h}$, offering a direct connection between far-ahead shadow rates and interest rates.[5] Further, assuming that the Fisher hypothesis holds, this connection gives $\bar{r}_t$ the interpretation of the median forecast of the real interest rate in the long run.[6] Notably, the same relationship holds for the medium–term yield in our model, up to a constant offset, because of the co-integrating relationship we have assumed. For the remainder of the paper, we refer to $\bar{r}_t$ as the trend real interest rate.

Importantly, the co-integrating relationship between the short–term interest rate and the medium–term yield in our model allows the medium–term yield to offer direct evidence on $\bar{r}_t$. This disciplines movements in $\bar{r}_t$ because the medium–term yield is above the ELB throughout our sample.

[5] In our model in section (2.2) $\lim_{h\to\infty} E_t\left(i_{t+h}\right) > \lim_{h\to\infty} E_t\left(s_{t+h}\right)$. However, one could conceptualize models in which it need not be strict.

[6] So long as $\bar{s}_t \geq 0$, which it is in our estimates, then our interpretation of $\bar{r}_t$ applies. However, if $\bar{s}_t < 0$, then the median forecast of the $\lim_{h\to\infty} i_{t+h} - \pi_{t+h}$ is $ELB - \bar{\pi}_t$. Then $\bar{r}_t$ would help determine the probability that interest rates would be above the ELB over the business cycle and would be less than the long–run median real interest rate.

2.5 Estimation Procedure

To estimate the parameters and unobserved states of the model, we use Bayesian methods.[7] The novel modeling contribution of this paper lies in the sampling of the unobserved trend and gap components of the data when the interest rate data are at the ELB, so we focus the text on this step of the estimation procedure. Conditional on parameter values and a sequence of volatilities, our model can be put into the form

$$\boldsymbol{\xi}_t = \boldsymbol{\mathcal{A}}\boldsymbol{\xi}_{t-1} + \boldsymbol{\mathcal{B}}_t\boldsymbol{\varepsilon}_t \tag{10}$$

$$\boldsymbol{X}_t = \boldsymbol{\mathcal{C}}\boldsymbol{\xi}_t \tag{11}$$

$$i_t = \max(s_t, ELB) \tag{12}$$

where $\boldsymbol{X}_t \equiv [s_t, y_t, \pi_t, \tilde{u}_t]'$, ε_t is a vector of standard normal random variables, ξ_t contains the stochastic trend and cyclical components of our model, as well as the appropriate number of lags, the matrices $\boldsymbol{\mathcal{A}}$, $\{\boldsymbol{\mathcal{B}}_t\}_{t=1}^T$, and $\boldsymbol{\mathcal{C}}$ are constructed accordingly from the parameters and volatilities in our model,[8] and the $\max$ operator encodes the ELB in the observation equation for the interest rate. We set the value of the ELB to zero, and assume that the federal funds rate was at the ELB for every quarter in which the target range for the federal funds rate was 0 to 25 basis points throughout the quarter.

Our approach for drawing from the posterior of $\boldsymbol{\xi} \equiv [\boldsymbol{\xi}_1, \boldsymbol{\xi}_2, \ldots, \boldsymbol{\xi}_T]'$ is to first treat the interest rate data at the ELB as missing and take draws from the posterior distribution of $\boldsymbol{\xi}$, which is straightforward using standard filtering and smoothing techniques. Knowing that the interest rate is at the ELB (not simply missing) in period t amounts to knowing that the values of $\boldsymbol{\xi}_t$ that are consistent with the data imply values of s_t that are less than the effective lower bound during that period. Thus, we can draw from the posterior of $\boldsymbol{\xi}$ by first treating interest rate data at the ELB as missing, and then rejecting draws until we find a $\boldsymbol{\xi}$ that is consistent with the ELB.

Our estimation procedure is a generalization of Park et al. (2007) that applies the method-

[7] Our data are quarterly, and we include two lags in $\boldsymbol{A}(L)$.

[8] In Appendix A we show how $\boldsymbol{\mathcal{A}}$ and $\boldsymbol{\mathcal{C}}$ can easily be made time–varying.

ology of Hopke et al. (2001). Appendix A explains in further detail how to construct a draw from the posterior distribution of ξ, conditional on the data, in a conditionally–linear Gaussian state–space model like ours. With a draw of ξ in hand, the posterior distribution of the parameters can be sampled using standard methods in the literature on conditionally–linear time series models with time–varying parameters and stochastic volatility, such as those used in Primiceri (2005) or Cogley and Sargent (2005b). We jointly estimate the parameters and unobserved states of the model using Bayesian MCMC techniques; our priors and details of the MCMC steps are described in Appendix B.

3 Shadow Rate and Trend Estimates

In this section we describe the posterior distribution of our model with regard to estimated shadow rates and trends. Our model is estimated using quarterly data from 1960:Q1 to 2015:Q4, which includes the recent period at the ELB. All data are publicly available from the FRED database maintained by the Federal Reserve Bank of St. Louis. Inflation is measured by the quarterly rate of change in the PCE headline deflator (expressed as an annualized percentage rate). Readings for the federal funds rate and the 5-year nominal bond yields are constructed as quarterly averages of the effective federal funds rate and the Treasury's 5-year constant maturity rate, respectively. The unemployment gap is computed as the difference between the quarterly average rate of unemployment and the CBO's measure of the natural long–term rate of unemployment for a given quarter. All computations are based on the vintage of FRED data available that has been available at the end of January 2016.[9] Figure 1 displays the data series we use for estimation, along with our estimated trends and corresponding uncertainty bands.

[Figure 1 about here.]

[9] See `https://research.stlouisfed.org/fred2/`. The PCE headline deflator is available at `https://research.stlouisfed.org/fred2/data/PCECTPI.txt`. The daily federal funds rate and the constant–maturity 5–year Treasury yield are available at `https://research.stlouisfed.org/fred2/data/DFF.txt` and `https://research.stlouisfed.org/fred2/data/GS5.tx`. The unemployment rate and the CBO's estimate of the natural rate of unemployment in the long run are available at `https://research.stlouisfed.org/fred2/series/UNRATE` and `https://research.stlouisfed.org/fred2/series/NROU`.

3.1 The Shadow Rate

Our model delivers estimates of the shadow rate of interest that are, by construction, less than the ELB during the period in which the bound is binding. Panel (a) of Figure 2 shows our posterior estimates of the shadow rate, along with uncertainty bands. Our model estimates indicate that the shadow rate fell sharply in early 2009, and began moving up toward the ELB in early 2013. The last observation in our sample, 2015:Q4, coincides with the last quarter before short–term interest rate data in the U.S. has begun to rise again above the ELB in recent years. Indeed, our end-of-sample estimate puts the shadow rate for 2015:Q4 just below the ELB.

[Figure 2 about here.]

Panel (b) of Figure 2 shows the posterior estimate of the shadow rate when we treat the interest rate data as missing over the period in which the ELB binds. Interestingly, the ELB does not pose much of a binding constraint for our sampling technique from 2009-2013, because the model would have predicted shadow rates below the ELB, even without knowledge that the ELB was binding in the data. Starting in 2013, there is non-negligible mass above the ELB when we treat the data as missing, meaning that the information content in the fact that the ELB was binding is greatest in this part of the ELB sample. Notably, even at the end of our sample, the ELB is well within the uncertainty bands our model produces for the shadow rate when we treat the interest rate data as missing.

For comparison, Figure 3 shows the posterior mean of our shadow rate, along with uncertainty bands, on the same plot as estimates from Wu and Xia (2016), and Krippner (2013).[10] Two features are worth noting. First, our estimated shadow rate, which also conditions on the unemployment gap and inflation as business cycle indicators, is lowest during 2009, near the trough of the Great Recession, according to the NBER. By contrast, the other estimates reach low points much later. Second, all three estimates are remarkably similar at the end of 2015, just before the Federal Reserve's departure from the ELB, even though our model has access

[10]Measures of the shadow rate from Priebsch (2013) and Ichiue and Ueno (2013) are not shown because their sample ends in 2013. Their measures are qualitatively similar in that they reach low points well after the trough of the recent recession.

to many fewer yields, we do not impose the rigid cross–equation restrictions associated with no–arbitrage assumptions in the dynamic term–structure literature, and our data sample does not include the period of departure from the ELB.

[Figure 3 about here.]

3.2 The Real Rate in the Long Run

Figure 4 displays the posterior median of our estimates of the trend real rate, $\bar{r}_t$, along with uncertainty bands. Panel (a) of Figure 4 shows quasi real–time estimates of $\bar{r}_t$, which are conditioned solely on data through period t. Panel (b) of Figure 4 shows the smoothed estimates, in that the entire data sample is used to estimate the parameters and $\bar{r}_t$. Notably, the uncertainty bands surrounding our estimates of $\bar{r}_t$ are wide. This result is consistent with results reported by Hamilton et al. (2015), Kiley (2015), and Lubik and Matthes (2015).

[Figure 4 about here.]

For both the pseudo–real–time and the smoothed estimates, any estimated downward trend in the real rate started well before the onset of the Great Recession. Studies like Laubach and Williams (2015) and Lubik and Matthes (2015) also document downward trajectories in the trend real rate; however, our estimates do not dip nearly as much as their estimates. One reason for the differences is our inclusion of stochastic volatility, which allows for large movements in the gap components of our model in 2008 and 2009. Another is that our estimation procedure explicitly models the ELB. If we instead ignore the ELB and treat the interest rate data as observations, we estimate a lower trend nominal interest rate, shown in Figure 5. When the ELB is ignored, the model is unable to generate a large cyclical movement in interest rates because it sees the interest rate stop falling at the ELB. As a result the model has difficulty explaining the prolonged period at the ELB without changes in the trend nominal rate. One margin by which the trend nominal rate can change is the trend real rate. By contrast, our model is able to produce a large shadow–rate gap in 2009, which helps explain why observed nominal interest rates remained at the ELB.

[Figure 5 about here.]

3.3 The Effect of Including the Medium–Term Yield

The posterior distribution of the shadow–rate at the ELB is particularly informed by the inclusion of the medium–term yield in our model. When we estimate the model without a medium–term yield, our posterior distribution of the shadow rate, shown in Panel (a) of Figure 6, is markedly more dispersed and lower on the eve of the Federal Reserve's departure from the ELB in 2015:Q4. The difference from our baseline model, which includes the medium–term yield, is particularly striking when we consider estimates that treat short–term rates as missing data during the ELB period, shown in Panel (b) of Figure 6, which is analogous to our discussion of Figure 2 above.

When shadow–rate estimates for the ELB period are solely informed by data on inflation and the unemployment–rate gap (and interest rate data up to 2008), the model would have expected the ELB to bind only for a couple of years, starting to place substantial odds on positive shadow rates around 2011. In contrast, when the medium–term yield is included in the estimation, the model predicts negative shadow rate at least until 2014, when short–term rate data is treated as missing as of 2009. Inclusion of the medium–term yield in our baseline model thus makes the ELB much less binding for our sampling routine than in the model without. Insofar as medium-term yields embed information about expected future short rates, it makes sense that including a medium–term yield will greatly inform our shadow rate estimates. In the next section we show that our model with the medium–term yield forecasts short–term interest rates largely better than the model without.

[Figure 6 about here.]

As shown in Panel (c) of Figure 6, the estimated trend real rate is fairly similar to our baseline estimates when the medium–term yield is excluded from the data. However, the estimated level of trend inflation is quite different, as shown in panel (d) of the figure. At the end of our sample, trend inflation derived from the model without the medium-term yield is markedly lower; which together with the mostly similar trend real rate implies a lower nominal short–term rate trend estimate in line with the model's lower estimate of the shadow rate trajectory shown in Panel (a). Overall, in the model without the medium–term yield, trend

inflation is more variable and more closely aligned with 4-quarter changes in the PCE headline deflator than in the baseline model as the presence of the medium-term yield helps the model to rationalize a more persistent inflation gap process.

4 Forecasting Interest Rates

Our shadow–rate approach has significant implications for forecasting interest rates. In this section we offer a number of ways to evaluate our shadow–rate approach by analyzing the model's out–of–sample predictions.

4.1 Predictive Density at Selected Dates

To create out–of–sample forecasts from our model, at each date we use the predictive densities from the posterior distribution (using data only up to that date) to forecast future interest rates. Our forecasting procedure thus captures uncertainty about both the parameter values and the unobserved states in our model; details are described in Appendix C. We compare these forecasts to the forecasts from the model when we ignore the ELB and feed the interest rate data into the model without accounting for the ELB.

[Figure 7 about here.]

The left panels of Figure 7 display statistics from the posterior predictive density of the short–term nominal interest rate from our baseline model at different dates. The forecast horizon extends for five years, and, in addition to mean and median predictions, shaded areas indicate 50 and 90 percent uncertainty bands. The dashed lines that extend below the ELB indicate posterior quantiles of the shadow rate distribution (as opposed to the interest rate distribution). The predictive density of the interest rate is a truncated version of the predictive density of the shadow rate distribution, so the quantiles of the shadow rate distribution become exactly the quantiles of the interest rate distribution if the value is larger than the ELB. The truncation of the shadow–rate distribution causes substantial asymmetry in the interest rate

distribution leading to marked differences in the predictive means and medians of our baseline model.

The right panels of Figure 7 display statistics from the posterior predictive density of the short–term nominal interest rate when we ignore the ELB. Here, the predicted interest rate distribution can have negative support because the ELB is ignored. Because the posterior distribution of the shadow rate is roughly symmetric in our model, the posterior predictive mean and median do not differ when we ignore the ELB.

In 2008:Q4, the first period before the ELB (Panels (a) and (b) of Figure 7), the model that ignores the ELB delivers the same forecasts for the shadow rates as our baseline model because there have been no ELB periods in the estimation and all interest rate data in the sample have been positive. When the ELB is ignored, shadow–rate forecasts are interest rate forecasts, and the model predicts future negative rates due to the substantial decline in real activity. Our baseline model takes the ELB into account and truncates the distribution of expected future shadow rates to produce interest rate forecasts. In doing so, the mean interest–rate forecast rises appreciably above the median for several periods.

In 2009:Q1, the period the ELB begins to bind (Panels (c) and (d) of Figure 7), the model that ignores the ELB produces a different predictive density for the shadow rate than our baseline model. The reason is that we allow lagged shadow rates to dynamically affect the current shadow rate. When we ignore the ELB, the lagged shadow rate is the lagged interest rate, which is higher in this period than our estimated shadow rate because of the ELB. This shifts up the distribution of expected shadow rates relative to our baseline model, producing notably more probability of positive interest rates in the subsequent few quarters even as the model predicts negative interest rates. As shown in Panel (c), accounting for the ELB produces interest rate forecasts that place substantial probability on remaining exactly at the ELB for several quarters. As in Panel (a), the truncation of the shadow rate distribution in order to produce interest rate forecasts creates a divergence of mean and median estimates of interest rates for several years.

[Figure 8 about here.]

In 2010:Q4, after the ELB had been binding for some time (panel (a) of figure 8), our baseline model still predicts substantial probability of interest rates at the ELB because of the estimated negative shadow rate. Moreover, the median interest rate forecast remains at the ELB for a number of quarters. By contrast, when the ELB is ignored (panel (b) of figure 8), the model predicts imminent departure from the effective lower bound because it does not estimate negative shadow rates and instead includes lagged observed interest rates in the dynamic system, which by construction are higher than our baseline model's estimated shadow rates. This difference persists throughout the ELB episode, leading to an extended period in which ignoring the ELB in the estimation of our model would lead one to predict immediate departure from the ELB. Toward the end of our sample (2015:Q4, shown in panels (c) and (d) of Figure 8), the forecasts from the two models are similar, in large part because our estimated shadow rate is only slightly less than the ELB at that point.

4.2 Forecasting Performance

We utilize the posterior predictive densities to calculate summary statistics in order to assess the forecasting performance of our baseline model at its variants. We focus on three statistics: the root–mean–squared error, evaluated at the posterior predictive density's mean; the mean absolution deviation, evaluated at the posterior predictive density's median; and the predictive score of the posterior distribution (Geweke and Amisano, 2010). We use the mean forecast for the root–mean–squared error statistic because the mean forecast minimizes expected square loss, and we use the median forecast for the mean absolute deviation statistic because the median minimizes expected absolute loss. In addition to our baseline model, we consider the version of the model where the ELB is ignored and a version of the model that includes the ELB in the estimation but does not include the medium–term yield.[11]

Tables 1 and 2 display forecast evaluation statistics for each model variant during our sample period to 2007 (prior to the ELB) and post 2007 for forecasts of future short–term interest rates, as well as future medium–term yields. The statistics for our baseline model are

[11] In the version of the model that ignores the ELB, lagged interest rate data are treated as lagged shadow rates and interest rate forecasts do not account for the ELB, as in the right–hand panels of Figures 7 and 8.

shown as calculated. The statistics for the alternative model specifications are shown on a relative basis to the baseline model.

[Table 1 about here.]

A key message from Table 1 is that the inclusion of the medium–term yield appears to help for forecasting short–term interest rates before 2007. At the one–quarter horizon, we find statistically significant declines in forecast performance for all three of our statistics when exclude the medium–term yield from our model. Because there are no periods at the ELB prior to 2007, the root–mean–squared error and mean absolute deviation statistics are identical for the baseline model and the model where the ELB is ignored for predictions about both short–term rates and medium–term yields. However, the predictive score statistic indicates that ignoring the ELB hurts forecasting performance. The reason is that the predictive score statistic incorporates information about the entire posterior density. During periods in which the nominal interest rate was low (for example, in 2003), accounting for the ELB has non–negligible effects on the shape of the predictive density. The predictive score statistic accounts for this affect, and the results illustrate the benefits of accounting for the ELB for density forecasts even when the ELB does not yet bind for the observed data.

[Table 2 about here.]

During the sample that includes the ELB, our baseline model almost uniformly out performs the model that ignores the ELB when predicting future short–term interest rates, as indicated in Panel A of Table 2.[12] The baseline model does particularly well when evaluating forecasts based on the posterior median because this is often exactly at the ELB over the sample. At the 8–quarter horizon, ignoring the ELB appears to perform somewhat better for the root–mean–squared error statistic, though not in terms of average absolute deviation from the predictive median. This finding highlights the implications of using different forecast statistics in samples affected by the ELB. In particular, the use of mean or median forecasts should be

[12]Point forecasts from the alternative model that ignores the ELB turn out to be negative during the early stages of the ELB period in 2009. Even when these forecasts are set equal to the ELB, they are outperformed by our baseline model at similar significance levels both in terms of *RMSE* and *MAD*.

carefully chosen for the relevant application in a model like ours. For forecasting short–term interest rates, during the sample that starts after 2007, our baseline model performs similarly to the model without the medium–term yield. The reason is that both models predict substantial probability of remaining at the ELB because each model produces estimates of the shadow rate that are less than zero.

Panel B of Table 2 displays our forecast evaluation statistics for forecasts of the medium–term yield during the sample that starts in 2008. For each statistic, our baseline model performs statistically better than the version that ignores the ELB for one–quarter ahead forecasts. The predictive score statistic also shows that accounting for the ELB improves forecasting performance over each of the next four quarters. Thus, our estimates indicate that information about short–term rates and medium–term yields jointly improve the forecasts of the other, meaning that the statistical connection is non–negligible and that accounting for the ELB improves density forecasts.

[Figure 9 about here.]

4.3 Forecast Uncertainty

Naturally, the ELB has important effects on the predictive density for nominal interest rates when the predictive density for shadow rates has non-negligible coverage below the ELB. To illustrate the relevance of these effects, Figure 9 compares forecast uncertainty in our baseline model against the alternative when the ELB is ignored. For the purpose of this figure, we measure forecast uncertainty by the conditional standard deviation of the predictive densities described above for the nominal short–term rate one and eight-quarters ahead. Overall, near– and medium–term uncertainty about future short–term rates has mostly declined since the mid-1980s. Nevertheless, as the level of nominal rates has been trending down over this period as well, the probability of reaching the ELB has become more and more non-negligible; this is particularly true for longer–horizons forecasts made since 2000, causing forecast uncertainty in the baseline model to differ from computations when the ELB is ignored.

Not surprisingly, the onset of the last NBER recession in 2007 is reflected in higher esti-

mated levels of stochastic volatility to all shocks in our model, leading to increased shadow–rate uncertainty. When the ELB is ignored, this directly translates into larger near–term uncertainty about the nominal short–term interest rate. By accounting for the ELB, our baseline model recognizes that during the last recession, increased shadow–rate uncertainty is accompanied by a marked downward shift of the shadow–rate distribution to values below the ELB such that the truncated distribution of actual nominal rates almost collapses at values at or slightly above the ELB. Consequently, near–term uncertainty for short–term nominal rates declines during the last recession when properly accounting for the ELB, as shown in Panel (a) of Figure 9. In contrast, as shown in Panel (b) of the figure, medium–term uncertainty about nominal interest rates increases with the increasing shadow–rate uncertainty, though not by quite as much, as nominal rates are projected to return to their estimated non–negative trend level.

5 Expected Interest Rate Paths

Our model's predicted paths for future short–term interest rates imply estimates of expected interest rate paths, and thus term–premiums for yields along the term–structure of interest rates. We define the expectations component of a yield on a bond with maturity h periods in the future as

$$e_{t,t+h} \equiv E_t \left(\frac{1}{h} \sum_{j=0}^{h-1} i_{t+j} \right).$$

The observed longer-term interest rate is given by

$$e_{t,t+h} + p_{t,t+h}$$

where $p_{t,t+h}$ represents premiums. Note that for any j, $E_t(i_{t+j}) \geq ELB$ and the posterior expectation can be constructed through simulation of the predictive density for nominal short–term interest rates as described in Appendix C.

[Figure 10 about here.]

We focus on the expectations component of the 5–year Treasury yield (y_t), which is in our data set. We construct the expectations component of y_t using the out–of–sample posterior predictive densities at time t. Figure 10 displays our estimated 5–year expectations component, along with uncertainty bands. Also shown are the expectations component from Kim and Wright (2005) as well as the 5–year Treasury yield in our data sample.

Despite not imposing the no–arbitrage cross–equation restrictions used in Kim and Wright (2005), our model produces similar estimates of the expectations component of the 5–year yield over the sample. The largest deviations are in the early 1990s and during the period in which the ELB binds. One advantage of our approach to modeling interest rates is that we can easily incorporate non–stationarity into the inflation process. Given that our estimated trend inflation rate has fallen since 1990, this may help explain why our estimates of the expectation component of the 5–year yield are higher than the estimates of Kim and Wright (2005), who assume that inflation is a stationary process. Interestingly, our model produces larger premiums than the model of Kim and Wright (2005) during the period in which the ELB binds. While the truncation of future shadow rates could have produced a higher expectations component for our model, it appears that the lagged shadow rates keep the interest rate low enough for long enough to produce relatively low paths for interest rates.

Notably, the uncertainty bands in Figure 10 are not of constant width. The stochastic volatility in our model leads to changes in the width of uncertainty bands, which is especially pronounced at the beginning of the Great Recession, a period in which our model estimates that volatility rose appreciably.

6 Conclusion

In this paper, we develop a methodology to account for the ELB in otherwise conditionally–linear Gaussian time series models. Further, we demonstrate how to estimate the parameters and latent states of such a model with an otherwise standard Bayesian MCMC sampler.

We document that including the ELB can have drastic effects for interest rate forecasts, as well as the expectations component of longer–term yields and thus also the computation of term–premiums. Further, accounting for the ELB using our shadow–rate approach appears to improve forecast performance. We also estimate changes in the trend real rate, defined as a long–term forecast of the real interest rate, and find that any decline in the trend real rate since the onset of the Great Recession is best characterized as a continuation of a downward trajectory that began well before.

APPENDIX

A Sampling States with Censored Data

Our Gibbs sampling procedure is a generalization of Park et al. (2007) that applies the methodology of Hopke et al. (2001). Assume that the vector $\boldsymbol{\xi}_t$ is a random variable that evolves so that

$$\boldsymbol{\xi}_t = \boldsymbol{\mathcal{A}}_t \boldsymbol{\xi}_{t-1} + \boldsymbol{\mathcal{B}}_t \boldsymbol{\varepsilon}_t \tag{13}$$

where $\boldsymbol{\varepsilon}_t$ is a vector of standard normal random variables of appropriate length and the sequence of matrices $\{\boldsymbol{\mathcal{A}}_t\}_{t=1}^T$ and $\{\boldsymbol{\mathcal{B}}_t\}_{t=1}^T$ are given.[13]

Define the vector

$$\boldsymbol{X}_t = \boldsymbol{\mathcal{C}}_t \boldsymbol{\xi}_t \tag{14}$$

where the sequence of matrices $\{\boldsymbol{\mathcal{C}}_t\}_{t=1}^T$ are known.[14] We assume that $\boldsymbol{X}_t$ has a partition made up of a vector shadow rates, $(\boldsymbol{S}_t)$, and a partition of variables that are unconstrained by

[13] In our application, described in the main body of the paper note that we have a constant $\boldsymbol{\mathcal{A}}_t = \boldsymbol{\mathcal{A}}$.
[14] In our application, described in the main body of the paper note that we have a constant $\boldsymbol{\mathcal{C}}_t = \boldsymbol{\mathcal{C}}$.

the ELB, $(\boldsymbol{M}_t)$.[15] That is,

$$\boldsymbol{X}_t = \begin{bmatrix} \boldsymbol{S}_t \\ \boldsymbol{M}_t \end{bmatrix} \tag{15}$$

The observed data are

$$\boldsymbol{Z}_t = \begin{bmatrix} \max\left(\boldsymbol{S}_t, ELB\right) \\ \boldsymbol{M}_t \end{bmatrix} \tag{16}$$

where the $\max$ operator is applied element by element. The ELB acts as a censoring function in the model through the $\max$ operator, though more general censoring functions could be used.

Define $\boldsymbol{X} \equiv [\boldsymbol{X}_1', \boldsymbol{X}_2', \ldots, \boldsymbol{X}_T']'$, and $\boldsymbol{Z} \equiv [\boldsymbol{Z}_1', \boldsymbol{Z}_2', \ldots, \boldsymbol{Z}_T']'$. We split $\boldsymbol{Z}$ into two parts, one part containing all non-interest rate data and all observations for interest rates that are not constrained by the ELB, $\boldsymbol{Z}^{NC}$, and another part with the interest rate data constrained at the ELB, $\boldsymbol{Z}^{C}$.[16] The corresponding elements of $\boldsymbol{X}$ are $\boldsymbol{X}^{NC}$ and $\boldsymbol{X}^{C}$. Note that, the elements of $\boldsymbol{X}^{C}$ are all shadow rates that are less than the ELB.

Given a normal distribution for $\boldsymbol{\xi}_0$, it follows that the vectors $\boldsymbol{X}^{NC}$ and $\boldsymbol{\xi} = [\boldsymbol{\xi}_1', \boldsymbol{\xi}_2', \ldots, \boldsymbol{\xi}_T']'$ have a multivariate normal (prior) distribution

$$\begin{bmatrix} \boldsymbol{X}^{NC} \\ \boldsymbol{\xi} \end{bmatrix} \sim N\left(\begin{bmatrix} \boldsymbol{\mu}_X \\ \boldsymbol{\mu}_\xi \end{bmatrix}, \begin{bmatrix} \boldsymbol{V}_{XX} & \boldsymbol{V}_{X,\xi} \\ \boldsymbol{V}_{\xi,X} & \boldsymbol{V}_{\xi,\xi} \end{bmatrix} \right) \tag{17}$$

and we can derive the posterior distribution for $\boldsymbol{\xi}$ conditional on observed interest rates, when the ELB is not binding, as well as all observations for macroeconomic, non-interest-rate variables $(\boldsymbol{M}_t)$:

$$\boldsymbol{\xi} \big| \left(\boldsymbol{X}^{NC} = \boldsymbol{Z}^{NC}\right) \sim N\left(\hat{\boldsymbol{\mu}}_\xi, \hat{\boldsymbol{V}}_{\xi,\xi}\right). \tag{18}$$

[15] In the application described above, there are in principle two shadow rates, one associated with the short–term interest rate and one associated with the medium–term yield described; in practice, the ELB constraint has been binding only for the former, however.

[16] Accordingly, $\boldsymbol{Z}^{C}$ consists solely of observations for interest rates that are equal to ELB.

In general, the posterior moments in (18) are given by

$$\hat{\boldsymbol{\mu}}_{\xi} = \boldsymbol{\mu}_{\xi} + \boldsymbol{K}\left(\boldsymbol{Z}^{NC} - \boldsymbol{\mu}_{X}\right) \qquad \text{with} \quad \boldsymbol{K} = \boldsymbol{V}_{\xi,X}\boldsymbol{V}_{XX}^{-1} \tag{19}$$

$$\text{and} \quad \hat{\boldsymbol{V}}_{\xi,\xi} = \boldsymbol{V}_{\xi,\xi} - \boldsymbol{V}_{\xi,X}\boldsymbol{V}_{XX}^{-1}\boldsymbol{V}_{X,\xi}\ . \tag{20}$$

Typically, these posterior moment matrices will by quite large; $\boldsymbol{\mu}_{\xi}$ is, for example, a vector of length $T \times N_{\xi} = 224 \times 12 = 2,688$ in our application, However, the Kalman smoother, adapted for handling missing observations for interest rates when the ELB binds, provides a convenient way to recursively compute the moments in (19) and (20) while recovering the distribution of $\boldsymbol{\xi}$ conditional on observations for $\boldsymbol{Z}^{NC}$. To this point, our procedure amounts to treating the observations for $\boldsymbol{Z}^{C}$ as missing data.[17]

We then note that the information contained in the interest rate data at the ELB is that $\boldsymbol{X}^{C} \leq ELB$ (for every element of $\boldsymbol{X}^{C}$). The posterior distribution of $\boldsymbol{\xi}$, conditional on $\boldsymbol{Z}$, is then

$$\boldsymbol{\xi}|(\boldsymbol{X} = \boldsymbol{Z}) \sim TN\left(\hat{\boldsymbol{\mu}}_{\xi}, \hat{\boldsymbol{V}}_{\xi,\xi}; \boldsymbol{X}^{C} \leq ELB\right) \tag{21}$$

where TN stands for a truncated normal such that its density function is

$$\Pr\left(\boldsymbol{\xi}|\boldsymbol{Z}\right) \propto \phi\left(\hat{\boldsymbol{\mu}}_{\xi}, \hat{\boldsymbol{V}}_{\xi,\xi}\right)\mathbf{1}(\boldsymbol{X}^{C} \leq ELB) \tag{22}$$

where ϕ is the multivariate normal density function and $\boldsymbol{X}^{C}$ is a shadow rate draw where every element is below the ELB. To sample from the posterior distribution of $\boldsymbol{\xi}$ conditional on all observations in $\boldsymbol{Z}$, we first draw $\boldsymbol{\xi}$ from $\Pr\left(\boldsymbol{\xi}\middle|\boldsymbol{X}^{NC} = \boldsymbol{Z}^{NC}\right)$. We then reject draws until we find a draw that satisfies the requirement that $\boldsymbol{X}^{C} \leq ELB$ for every element. Rejection sampling is thus done on an entire draw of $\boldsymbol{\xi}$, which corresponds to an entire draw of the time series for $\boldsymbol{\xi}_{t}$.

In our baseline framework, lagged values of $\boldsymbol{\xi}_{t}$ appear as explanatory variables and are not

[17] Alternatively, Chan and Jeliazkov (2009) describe ways to efficiently compute the moments in (19) and (20) based on sparse matrices that exploit the state space structure inherent in (17).

censored. A straightforward extension is to incorporate a given number of p lags of $\boldsymbol{Z}_t$, which includes interest rate data that can be constrained the ELB. In this case, we change (13) to be

$$\boldsymbol{\xi}_t = \boldsymbol{\mathcal{A}}_t \boldsymbol{\xi}_{t-1} + \boldsymbol{\mathcal{F}}_t \boldsymbol{\zeta}_{t-1} + \boldsymbol{\mathcal{B}}_t \boldsymbol{\varepsilon}_t \tag{23}$$

$$\boldsymbol{\zeta}_{t-1} \equiv [\boldsymbol{Z}'_{t-1}, \boldsymbol{Z}'_{t-2}, \ldots, \boldsymbol{Z}'_{t-p}]' \tag{24}$$

where $\{\boldsymbol{\mathcal{F}}_t\}_{t=1}^T$ are conformable matrices that are known. The posterior of $\boldsymbol{\xi}$ can be constructed exactly as in our baseline model, treating $\{\boldsymbol{\zeta}_{t-1}\}_{t=1}^T$ as exogenous in every period because the rejection step will ensure that the sampled values of $\boldsymbol{\xi}$ are consistent with $\boldsymbol{\zeta}_{t-1}$ for all t. For comparison, the models of Iwata and Wu (2006) and Nakajima (2011) can be cast, conditional on parameter values, as special cases of this setup in which the matrix $\boldsymbol{A}_t = \boldsymbol{0}$. A notable difference in the posterior simulation of the model is that the truncated distributions in Iwata and Wu (2006) and Nakajima (2011) can be cast as period–by–period truncated normals. By contrast, our posterior estimates require rejection sampling on an entire time series draw of $\boldsymbol{\xi}$.

B Priors and Posterior Sampling

MCMC estimates of the model are obtained from a Gibbs sampler. The sampler is run multiple times with different starting values and convergence is assessed with the scale reduction test of Gelman et al. (2003).[18] For each run, $20,000$ draws are stored after a burn-in period of $100,000$ draws; the post-burnin draws from each run are then merged.

Our models consist of two vectors of latent states:

$$\boldsymbol{\xi}_t = \begin{bmatrix} \bar{\pi}_t & \bar{r}_t & \bar{s}_t & \bar{y}_t & \tilde{\pi}_t & \tilde{u}_t & \tilde{s}_t & \tilde{y}_t & e_{\pi,t} \end{bmatrix}'$$

$$\text{and} \quad \boldsymbol{h}_t = \begin{bmatrix} \log(\sigma^2_{\bar{\pi},t}) & \log(\sigma^2_{\bar{\pi},t}) & \log(\sigma^2_{\bar{u},t}) & \log(\sigma^2_{\bar{s},t}) & \log(\sigma^2_{\bar{y},t}) & \log(\sigma^2_{e,t}) \end{bmatrix}'$$

[18] Specifically, for every model, 10 independent runs for the Gibbs sampler were evaluated; each run initialized with different starting values drawn from the model's prior distribution. Convergence is deemed satisfactory when the scale reduction statistics for every parameter and latent variable are below 1.2; (values close to 1 indicate good convergence).

as well as the parameters governing the means and volatility of shocks to $\boldsymbol{h}_t$, see (7), stacked in the vectors $\boldsymbol{\mu}$ and $\boldsymbol{\phi^2}$,[19] the variance of shocks to the trend real rate, denoted $\sigma^2_{\bar{r}}$, the transition coefficients of the gap VAR (6), stacked in a vector $\boldsymbol{a}$, and lower diagonal elements of gap shock loadings $\boldsymbol{B}$ in (6) that can be stacked in a vector denoted $\boldsymbol{b}$. For ease of reference, all parameters are collected in the vector $\boldsymbol{\theta} = \begin{bmatrix} \boldsymbol{a}' & \boldsymbol{b}' & \sigma^2_{\bar{r}} & \boldsymbol{\phi^{2\prime}}, & \boldsymbol{\mu}' \end{bmatrix}'$. Furthermore, since MCMC estimates of $\boldsymbol{h}^T$ will be obtained from the multi–move filter of Kim et al. (1998), the use of a set of discrete indicator variables, $\boldsymbol{s^T}$, is required to to approximate $\log \eta^2_{j,t}$ in (7) with a mixture of normals. Conditional on draws for the parameters, ($\boldsymbol{\theta}$), and log-volatilities $\boldsymbol{h}^T$, we can construct matrices $\boldsymbol{\mathcal{A}}$, $\{\boldsymbol{\mathcal{B}}_t\}_{t=1}^T$, and $\boldsymbol{\mathcal{C}}$ and to obtain the linear, Gaussian state space system described by equations (13) and (14) in Appendix A.

For the initial values of the latent states, the following priors were used:

$$\boldsymbol{\xi_0} \sim N\left(E(\boldsymbol{\xi}_0), \boldsymbol{\Omega}\right) \qquad \text{with} \quad E(\boldsymbol{\xi}_0) = \begin{bmatrix} \bar{\boldsymbol{\xi}} \\ \mathbf{0} \end{bmatrix} \qquad \text{and} \quad \boldsymbol{\Omega} = \begin{bmatrix} \bar{\boldsymbol{\Omega}} & \mathbf{0} \\ \mathbf{0} & \tilde{\boldsymbol{\Omega}} \end{bmatrix} \tag{25}$$

An uninformative prior for the initial gap levels is obtained by setting $\tilde{\boldsymbol{\Omega}}$ equal to the ergodic variance-covariance matrix of the gaps implied by the VAR (6), evaluated at the time zero draws for the stochastic volatilities, encoded in $\boldsymbol{\Sigma}_0$, for every MCMC draw.[20] The prior for the initial trend levels are set to be consistent with

$$\begin{bmatrix} \bar{\pi}_0 \\ \bar{s}_0 \\ \bar{y}_0 \end{bmatrix} \sim N\left(\begin{bmatrix} 2 \\ 4 \\ 5 \end{bmatrix}, \begin{bmatrix} 16 & -16 & -16 \\ -16 & 116 & 16 \\ -16 & 16 & 116 \end{bmatrix} \right) \tag{26}$$

which implies a fairly vague prior level of the real-rate trend, $\bar{r}_t = \bar{s}_t - \bar{\pi}_t$ while taking correlated signals about the initial level of trend inflation from readings on all three nominal variables.

[19] The auto-regressive coefficients ρ_j in each of the stochastic volatility equations in (7) are fixed at 0.99.

[20] In the case of a VAR(1), the ergodic variance-covariance matrix solves $\tilde{\boldsymbol{\Omega}} = \boldsymbol{A}\tilde{\boldsymbol{\Omega}}\boldsymbol{A}' + \boldsymbol{B}\,\boldsymbol{\Sigma}_0\,\boldsymbol{B}'$ for given values of $\boldsymbol{A}$, $\boldsymbol{B}$, and $\boldsymbol{\Sigma}_0$.

The prior for the average level of the log-variances is:

$$\mu_j \sim N\left(2 \cdot \log \frac{1}{10} - \frac{25}{4}, 25\right) \qquad \Rightarrow E(\bar{\sigma}_t) = \frac{1}{10} \tag{27}$$

The prior distribution for each of the the parameters for the parameters $\boldsymbol{\phi^2}$ is a univariate inverse–Wishart distribution with 30 degrees of freedom (corresponding to an inverse gamma with a shape parameter set equal to a value of 15) and a mean equal to 0.2^2 which coincides with the fixed coefficient-value of 0.2 used by Stock and Watson (2007) in their univariate model for inflation.

The parameter governing the variability of real-rate trend shocks, $\sigma^2_{\tilde{r}}$, has a univariate inverse–Wishart distribution with 3 degrees of freedom (corresponding to an inverse–gamma distribution with a shape parameter equal to 1.5 degrees of freedom) and is centered around a prior mean of 0.2^2. While this vaguely informative prior embeds the belief that the trend shocks explain only a small share of variations in real rates, it also helps to avoid the pile–up problem — known, for example, from Stock and Watson (1998) and considered in the context of estimating $\sigma^2_{\tilde{r}}$ also by Laubach and Williams (2003) as well as Clark and Kozicki (2005) — by keeping posterior draws for the parameter away from zero.

While the priors for $\boldsymbol{a}$ and $\boldsymbol{b}$ are taken to be completely diffuse, starting values for the Gibbs sampler are drawn from the following normal distributions:

$$\boldsymbol{a} \sim N\left(\mathbf{0}, 0.3^2 \cdot \boldsymbol{I}\right) \qquad \boldsymbol{b} \sim N\left(\mathbf{0}, \boldsymbol{I}\right) \tag{28}$$

The Gibbs sampler is initialized with values drawn from the prior for $\boldsymbol{h}^T$ and $\boldsymbol{\theta}$ and then generates draws from the joint posterior distribution

$$p\left(\boldsymbol{\xi}^T, \boldsymbol{h}^T, \boldsymbol{a}, \boldsymbol{b}, \sigma^2_{\tilde{r}}, \boldsymbol{\mu}, \boldsymbol{\phi^2}, s^T \middle| \boldsymbol{Y^T}\right)$$

by iterating over draws from the following conditional distributions:

1. Draw from $p\left(\boldsymbol{\xi}^T \middle| \boldsymbol{h}^T, \boldsymbol{a}, \boldsymbol{b}, \sigma^2_{\tilde{r}}, \boldsymbol{\phi^2}, \boldsymbol{\mu}, Y^T\right)$ with the disturbance smoothing sampler of Durbin and Koopman (2002) and rejection sampling for the shadow rate when the ob-

served nominal short–term rate is at the ELB as described in Appendix A.

2. Draw from $p\left(\boldsymbol{a}\middle|\boldsymbol{\xi}^T,\boldsymbol{h}^T,\boldsymbol{b},\sigma_{\bar{r}}^2,\boldsymbol{\phi^2},\boldsymbol{\mu},Y^T\right)=p\left(\boldsymbol{a}\middle|\boldsymbol{\xi}^T,\boldsymbol{h}^T,\boldsymbol{b}\right)$, a normal conjugate posterior for a VAR with known heteroscedasticity, with rejection sampling to ensure a stationary VAR (Cogley and Sargent, 2005a; Clark, 2011)

3. Draw from $p\left(\boldsymbol{b}\middle|\boldsymbol{\xi}^T,\boldsymbol{h}^T,\boldsymbol{a},\sigma_{\bar{r}}^2,\boldsymbol{\phi^2},\boldsymbol{\mu},Y^T\right)$ via recursive Bayesian regressions with known heteroscedasticity to orthogonalize the gap shocks of the VAR in (6).

4. Draw from the inverse-gamma conjugate posteriors for $\sigma_{\bar{r}}^2$:

$$p\left(\sigma_{\bar{r}}^2\middle|\boldsymbol{\xi}^T,\boldsymbol{h}^T,\boldsymbol{a},\boldsymbol{b},\boldsymbol{\phi^2},\boldsymbol{\mu},Y^T\right)=p\left(\sigma_{\bar{r}}^2\middle|\boldsymbol{\xi}^T\right)$$

5. Draw from the inverse-gamma conjugate posteriors for $\boldsymbol{\phi^2}$:

$$p\left(\boldsymbol{\phi^2}\middle|\boldsymbol{\xi}^T,\boldsymbol{h}^T,\boldsymbol{a},\boldsymbol{b},\sigma_{\bar{r}}^2,\boldsymbol{\mu},Y^T\right)=p\left(\bar{\phi}^2\middle|\boldsymbol{h}^T\right)$$

6. Draw the mixture indicators s^T from:

$$p\left(s^T\middle|\boldsymbol{\xi}^T,\boldsymbol{h}^T,\boldsymbol{a},\boldsymbol{b},\sigma_{\bar{r}}^2,\boldsymbol{\phi^2},\boldsymbol{\mu},Y^T\right)$$

7. Draw from $p\left(\boldsymbol{h}^T,\boldsymbol{\mu}\middle|s^T,\boldsymbol{\xi}^T,\boldsymbol{a},\boldsymbol{b},\sigma_{\bar{r}}^2,\boldsymbol{\phi^2},Y^T\right)=p\left(\boldsymbol{h}^T\middle|s^T,\boldsymbol{\xi^T},\bar{\phi}^2\right)$ embedding the disturbance smoothing sampler of Durbin and Koopman (2002) in a linear state space for $\left(\boldsymbol{h}^T,\boldsymbol{\mu}\right)$ as in Kim et al. (1998).[21]

Strictly speaking, this is not a simple Gibbs sampler consisting of steps 1 – 7, but rather a Gibbs-within-Gibbs sampler with the outer Gibbs sampler iterating between

$$p\left(s^T,\boldsymbol{\xi}^T,\boldsymbol{\theta}\middle|\boldsymbol{h}^T,Y^T\right) \quad \text{(thus, a block consisting of steps 1 through 6)}$$

and $$p\left(\boldsymbol{h}^T,\boldsymbol{\mu}\middle|s^T,\boldsymbol{\xi}^T,\boldsymbol{a},\boldsymbol{b},\sigma_{\bar{r}}^2,\boldsymbol{\phi^2},Y^T\right) \quad \text{(step 7),}$$

similar to the discussion by Del Negro and Primiceri (Forthcoming).

[21] The constant $\boldsymbol{\mu}$ is embedded in the state space as a unit root without shocks, which improves the efficiency of the Gibbs sampler by jointly sampling $\boldsymbol{h}^T$ and $\boldsymbol{\mu}$.

C Computation of Predictive Densities

In order to derive predictive densities for interest rates (and other data in $\boldsymbol{Z}_t$), we first proceed by characterizing the predictive density for the shadow rate, included in the non-censored vector of variables $\boldsymbol{X}_t$ described in Appendix A. Apart from handling the truncation issues related to the ELB, our approach is fairly standard, building, for example, on the work by Geweke and Amisano (2010), Christoffel et al. (2010), and Warne et al. (2015). Given the truncation issues for interest rates and the fat tails introduced into the predictive density by the stochastic volatility specification, we have chosen to compute the predictive density based on the mixture of normals that is implied by the draws from our MCMC sampler, instead of approximating the predictive density solely based on its first two moments, treating the predictive density as a normal distribution, as has been done, for example, by Adolfson et al. (2007) in the case of linearized, constant-parameter DSGE models.

In order to compute the predictive density for $\boldsymbol{Z}_{t+h}$ jumping off data at time t, we first employ the MCMC sampler described in Appendix B to re-estimate all model parameters and latent variables ($\boldsymbol{\theta}$, $\boldsymbol{\xi}_{1:t}$ and $\boldsymbol{h}_{1:t}$) conditional on data available through time t. Draws from this MCMC sampler will henceforth be indexed by k.

Conditional on draws $(\boldsymbol{\xi}_t^k, \boldsymbol{h}_t^k, \boldsymbol{\theta}^k)$, it is straightforward to compute the predictive mean for uncensored variables:

$$E\left(\boldsymbol{X}_{t+h}|\boldsymbol{\xi}_t^k, \boldsymbol{h}_t^k, \boldsymbol{\theta}^k\right) = \boldsymbol{C}^k \left(\boldsymbol{\mathcal{A}}^k\right)^h \boldsymbol{\xi}_t^k \tag{29}$$

and the predictive mean, conditional solely on data through t, can then be approximated by averaging over the means derived from each MCMC draw:

$$E\left(\boldsymbol{X}_{t+h}|\boldsymbol{Z}_{1:t}\right) \approx \sum_k E\left(\boldsymbol{X}_{t+h}|\boldsymbol{\xi}_t^k, \boldsymbol{h}_t^k, \boldsymbol{\theta}^k\right) \tag{30}$$

However, in order to characterize the entire predictive density for uncensored variables or even the predictive density for interest rates, which are subject to censoring due to the ELB constraint, we need to account for non-linearities in the distribution for future $\boldsymbol{\xi}_{t:t+h}$ arising

from the stochastic volatility shocks in our model. To do so, we simulate $J = 100$ trajectories, each indexed by j, of $\boldsymbol{h}_{t:t+h}^{k,j}$ for each draw k from the MCMC sampler. Conditional on $(\boldsymbol{\xi}_t^k, \boldsymbol{h}_t^k, \boldsymbol{\theta}^k)$ as well as $\boldsymbol{h}_{t:t+h}^{k,j}$, $\boldsymbol{\xi}_{t:t+h}$ and $\boldsymbol{X}_{t:t+h}$ are normally distributed. The means of the conditional normals are still given by (29), and the variances are given by

$$\text{Var}\left(\boldsymbol{\xi}_{t+h}|\boldsymbol{\xi}_t^k, \boldsymbol{h}_t^k, \boldsymbol{h}_{t+1:t+h}^{k,j}, \boldsymbol{\theta}^k\right) = \sum_{i=0}^{h} \left(\boldsymbol{\mathcal{A}}^k\right)^i \boldsymbol{\Sigma_{t+i}}^{k,j} \left(\left(\boldsymbol{\mathcal{A}}^k\right)^i\right)' \tag{31}$$

$$\text{Var}\left(\boldsymbol{X}_{t+h}|\boldsymbol{\xi}_t^k, \boldsymbol{h}_t^k, \boldsymbol{h}_{t+1:t+h}^{k,j}, \boldsymbol{\theta}^k\right) = \boldsymbol{\mathcal{C}}^k \,\text{Var}\left(\boldsymbol{\xi}_{t+h}|\boldsymbol{\xi}_t^k, \boldsymbol{h}_t^k, \boldsymbol{h}_{t+1:t+h}^{k,j}, \boldsymbol{\theta}^k\right) \left(\boldsymbol{\mathcal{C}}^k\right)' \tag{32}$$

Recall that $\boldsymbol{X}_{t:t+h}$ contains shadow rates $\boldsymbol{S}_{t:t+h}$ and the predictive density for nominal interest rates can be constructed by computing the moments and density function of the truncated normal distribution conditional on every pair of draws (k, j). Specifically, consider the short–term shadow rate s_{t+h} and denote its conditional predictive mean and variance for draw (k, j), computed according to (29) and (32), by $m^{k,j} = m^k$ and $v^{k,j}$. The predictive density for $i_t = \max(s_t, ELB)$, conditional on draw (k, j), is then characterized by:

$$P^{k,j} \equiv Pr(s_{t+h} < ELB|\cdot) \tag{33}$$

$$p^{k,j} \equiv \phi(s_{t+h} < ELB|\cdot) \tag{34}$$

$$E\left(i_{t+h}|\cdot\right) = P^{k,j} \cdot ELB + (1 - P^{k,j}) \cdot \left(m^{k,j} + \sqrt{v^{k,j}}\,\frac{p^{k,j}}{P^{k,j}}\right) \tag{35}$$

$$\text{Var}\left(i_{t+h}|\cdot\right) = (1 - P^{k,j}) \cdot v^{k,j} \left(1 + \frac{(ELB - m^{k,j})p^{k,j}}{\sqrt{v^{k,j}}\,P^{k,j}} + \left(\frac{p^{k,j}}{P^{k,j}}\right)^2\right) \tag{36}$$

$$f\left(i_{t+h}|\cdot\right) = \mathbf{1}(i_{t+h} = ELB)P^{k,j} \ldots + \tag{37}$$

$$+ \mathbf{1}(i_{t+h} > ELB)(1 - P^{k,j}) \cdot \frac{\phi\left((i_{t+h} - m^{k,j})/\sqrt{v^{k,j}}\right)}{\sqrt{v^{k,j}}\,P^{k,j}} \tag{38}$$

where "$\cdot$" in "$(i_{t+h}|\cdot)$" is a placeholder for the conditioning set $\left(\boldsymbol{\xi}_t^k, \boldsymbol{h}_t^k, \boldsymbol{h}_{t+1:t+h}^{k,j}, \boldsymbol{\theta}^k\right)$, and $\phi(\cdot)$ is the standard normal pdf.

Based on these conditional distribution for every draw (k, j) we construct predictive means and variances by aggregating across draws using the law of iterated expectations and the law of

total variance, respectively. Predictive medians are obtained from simulated draws of i_{t+h} for every draw (k, j) and computing the 50% quantile across all draws. The time t contribution to the predictive scores are computed from averaging across draws the conditional likelihoods $f\left(i_{t+h}|\cdot\right)$; as in Geweke and Amisano (2010) the predictive score for an evaluation window ranging from $t = T_1$ through $t = T_2$ is then given as

$$PS = \frac{1}{T_2 - T_1 + 1} \sum_{t=T_1}^{T_2} \log f\left(i_{t+h}|\boldsymbol{Z}_{0:t}\right) . \tag{39}$$

References

Malin Adolfson, Jesper Linde, and Mattias Villani. Forecasting Performance of an Open Economy DSGE Model. *Econometric Reviews*, 26(2-4):289–328, 2007.

Michael D. Bauer and Glenn D. Rudebusch. Monetary policy expectations at the zero lower bound. *Federal Reserve Bank of San Francisco Working Paper Series*, 2014.

Stephen Beveridge and Charles R. Nelson. A new approach to decomposition of economic time series into permanent and transitory components with particular attention to measurement of the business cycle. *Journal of Monetary Economics*, 7(2):151–174, 1981.

Fischer Black. Interest rates as options. *The Journal of Finance*, 50(5):1371–1376, 1995.

John Y. Campbell and Robert J. Shiller. Cointegration and tests of present value models. *The Journal of Political Economy*, 95(5):1062–1088, October 1987.

John Y. Campbell and Robert J. Shiller. Yield spreads and interest rate movements: A bird's eye view. *The Review of Economic Studies*, 58(3):495–514, 1991.

Joshua C.C. Chan and Ivan Jeliazkov. Efficient simulation and integrated likelihood estimation in state space models. *International Journal of Mathematical Modelling and Numerical Optimization*, 1(1/2):101–120, 2009.

Joshua C.C. Chan and Rodney Strachan. The zero lower bound: Implications for modelling the interest rate. *Working Paper*, 2014.

Kai Christoffel, Anders Warne, and Gnter Coenen. Forecasting with DSGE models. Working Paper Series 1185, European Central Bank, May 2010.

Todd E. Clark. Real-time density forecasts from bayesian vector autoregressions with stochastic volatility. *Journal of Business & Economic Statistics*, 29(3):327–341, 2011.

Todd E. Clark and Sharon Kozicki. Estimating equilibrium real interest rates in real time. *The North American Journal of Economics and Finance*, 16(3):395–413, December 2005.

Timothey Cogley and Thomas J. Sargent. Measuring price level uncertainty and instability in the U.S., 1850–2012. *Review of Economics and Statistics*, Forthcoming.

Timothy Cogley and Thomas J. Sargent. Drift and volatilities: Monetary policies and outcomes in the post WWII U.S. *Review of Economic Dynamics*, 8(2):262–302, April 2005a.

Timothy Cogley and Thomas J. Sargent. Drifts and volatilities: monetary policies and outcomes in the post WWII US. *Review of Economic Dynamics*, 8(2):262–302, 2005b.

Marco Del Negro and Giorgio E. Primiceri. Time-varying structural vector autoregression and monetary policy: Corrigendum. *Review of Economic Studies*, Forthcoming.

Fancis X. Diebold and Canlin Li. Forecasting the term sturcutre of government bond yields. *Journal of Econometrics*, (130):337–364, 2006.

Francis X Diebold and Roberto S Mariano. Comparing predictive accuracy. *Journal of Business & Economic Statistics*, 13(3):253–63, July 1995.

J. Durbin and S. J. Koopman. A simple and efficient simulation smoother for state space time series analysis. *Biometrika*, 89(3):603–615, September 2002.

Andrew Gelman, John B. Carlin, Hal S. Stern, and Donald B. Rubin. *Bayesian Data Analysis*. Chapman and Hall, 2nd edition, 2003.

John Geweke and Gianni Amisano. Comparing and evaluating bayesian predictive distributions of asset returns. *International Journal of Forecasting*, 26(2):216–230, 2010. Special Issue: Bayesian Forecasting in Economics.

James D. Hamilton, Ethan S. Harris, Jan Hatzius, and Kenneth D. West. The equilibrium real funds rate: Past, present and future. *Working Paper*, March 2015.

Philip K. Hopke, Chuanhai Liu, and Donald B. Rubin. Multiple imputation for multivariate data with missing and below-threshold measurements: Time-series concentrations of pollutants in the arctic. *Biometrics*, 57(1):22–33, 2001. ISSN 0006341X.

Hibiki Ichiue and Yoichi Ueno. Estimating term premia at the zero bound: An analysis of Japanese, US, and UK yields. Working Paper Series 2013–E–8, Bank of Japan, 2013.

Shigeru Iwata and Shu Wu. Estimating monetary policy effects when interest rates are close to zero. *Journal of Monetary Economics*, 53(7):1395 – 1408, 2006.

Michael T. Kiley. What can the data tell us about the equilibrium real interest rate? *Finance and Economics Disucssion Series*, (2015-77), 2015.

Don Kim and Kenneth J. Singleton. Term structure models and the zero bound: An emprirical investigation of Japanese yields. *Mimeo*, 2011.

Don H. Kim and Jonathan H. Wright. An arbitrage–free three–factor term strucutre model and the recent behavior of long–term yields and distant–horizon forward rates. *FEDS Working Paper Series*, 2005.

Sangjoon Kim, Neil Shephard, and Siddhartha Chib. Stochastic volatility: Likelihood inference and comparison with arch models. *The Review of Economic Studies*, 65(3):361–393, July 1998.

Robert G. King and André Kurmann. Expectations and the term structure of interest rates: Evidence and implications. *Federal Reserve Bank of Richmond Economic Quarterly*, (Fall): 49–95, August 2002.

Leo Krippner. Measuring the stance of monetary policy in zero lower bound environments. *Economics Letters*, 118(1):135–138, 2013.

Leo Krippner. *Zero Lower Bound Term Structure Modeling: A practitioner's Guide*. Palgrave Macmillan, 2015.

Thomas Laubach and John C. Williams. Measuring the natural rate of interest. *The Review of Economics and Statistics*, 85(4):1063–1070, November 2003.

Thomas A. Laubach and John C. Williams. Measuring the natural rate of interest redux. *Hutchins Center on Fiscal & Monetary Policy at Brookings*, (15), 2015.

Marco Jacopo Lombardi and Feng Zhu. A shadow policy rate to calibrate US monetary policy at the zero lower bound. BIS Working Papers 452, Bank for International Settlements, June 2014.

Thomas A. Lubik and Christian Matthes. Calculating the natural rate of interest: A comparison of two alternative approaches. *Economic Brief*, (15-10), 2015.

Elmar Mertens. Measuring the level and uncertainty of trend inflation. Review of Economics and Statistics, forthcoming.

Jouchi Nakajima. Monetary policy transmission under zero interest rates: An extended time-varying parameter vector autoregression approach. *Bank of Japan Working Paper Series*, 2011.

Jung Wook Park, Marc G. Genton, and Sujit K. Ghosh. Censored time series analysis with autoregressive moving average models. *The Canadian Journal of Statistics / La Revue Canadienne de Statistique*, 35(1):151–168, 2007.

Marcel A. Priebsch. Computing arbitrage-free yields in multi-factor Gaussian shadow-rate term structure models. Finance and Economics Discussion Series 2013-63, Board of Governors of the Federal Reserve System (U.S.), 2013.

Giorgio E. Primiceri. Time varying structural vector autoregressions and monetary policy. *The Review of Economic Studies*, 72(3):821–852, 2005.

Lukasz Rachel and Thomas D. Smith. Secular drivers of the global real interest rate. *Bank of England Staff Working Paper*, (571), 2015.

Christopher A. Sims. Macroeconomics and reality. *Econometrica*, 48(1):1–48, 1980.

James H. Stock and Mark W. Watson. Median unbiased estimation of coefficient variance in a time-varying parameter model. *Journal of the American Statistical Association*, 93(441): 349–358, 1998.

James H. Stock and Mark W. Watson. Why has U.S. inflation become harder to forecast? *Journal of Money, Credit and Banking*, 39(S1):3–33, February 2007.

Lawrence H. Summers. Us economic prospects: Secular stagnation, hysteresis and the zero lower bound. *Buiness Economics*, 49(2):65–73, 2014.

Anders Warne, Gnter Coenen, and Kai Christoffel. Marginalized predictive likelihood comparisons of linear gaussian state-space models with applications to dsge, dsge-var, and var models. *mimeo* European Central Bank, December 2015.

Jing Cynthia Wu and Fan Dora Xia. Measuring the macroeconomic impact of monetary policy at the zero lower bound. *Journal of Money, Credit and Banking*, 48(2-3):253–291, 2016. ISSN 1538-4616. doi: 10.1111/jmcb.12300. URL `http://dx.doi.org/10.1111/jmcb.12300`.

Figure 1: Data and Estimated Trends

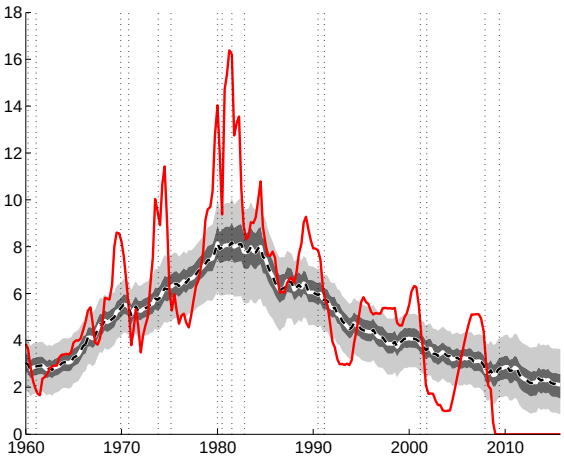

(a) Federal Funds Rate

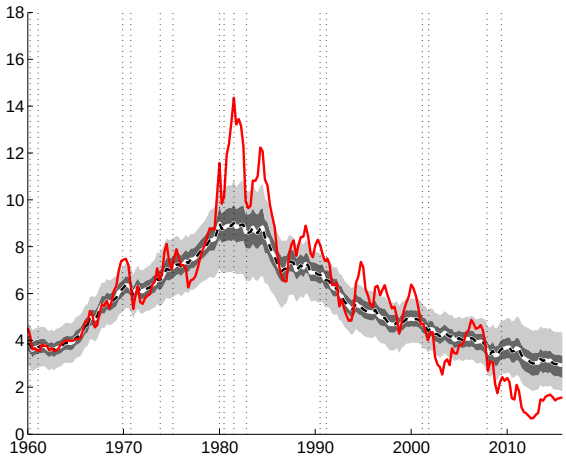

(b) 5–Year Treasury Yield

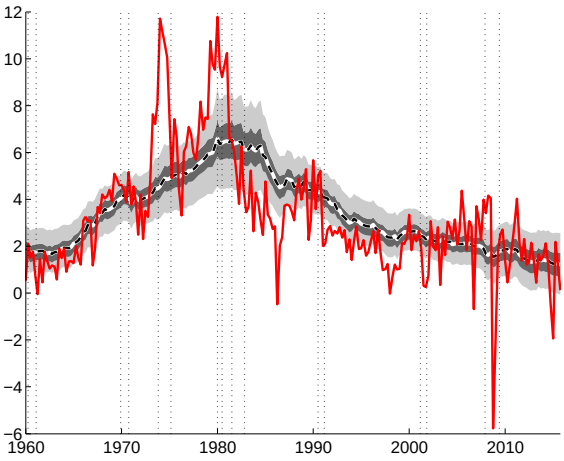

(c) PCE Inflation Rate

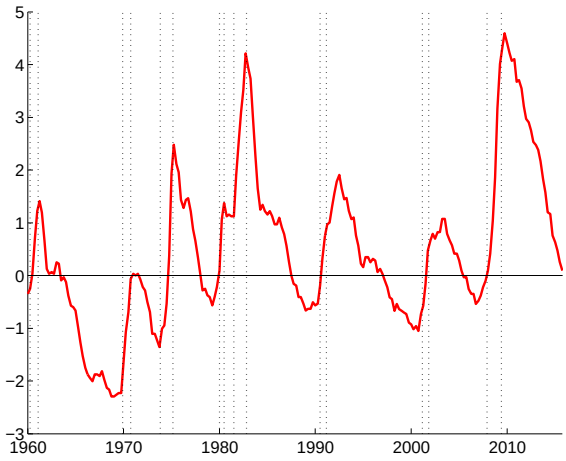

(d) Unemployment–Rate Gap

Note: Red solid lines are data. Shaded areas indicate 50 and 90 percent uncertainty bands, dashed lines are posterior means. The posterior distribution is derived from conditioning the model on the entire data sample 1960:Q1 – 2015:Q4. Uncertainty bands reflect the joint uncertainty about model parameters and states. Dotted vertical lines indicate NBER recession peaks and troughs. Data source: Federal Reserve Bank of St. Louis, Federal Reserve Economic Data (FRED), and Congressional Budget Office.

Figure 2: Shadow Rate Estimates

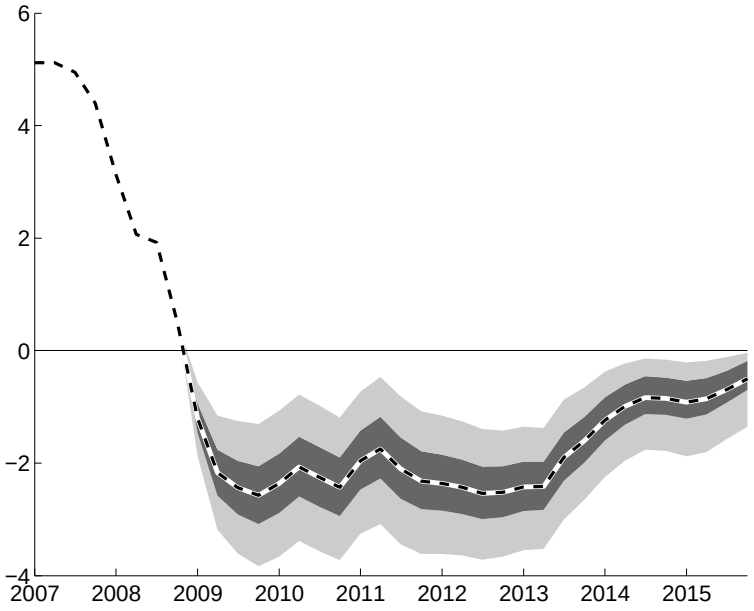

(a) Baseline Model

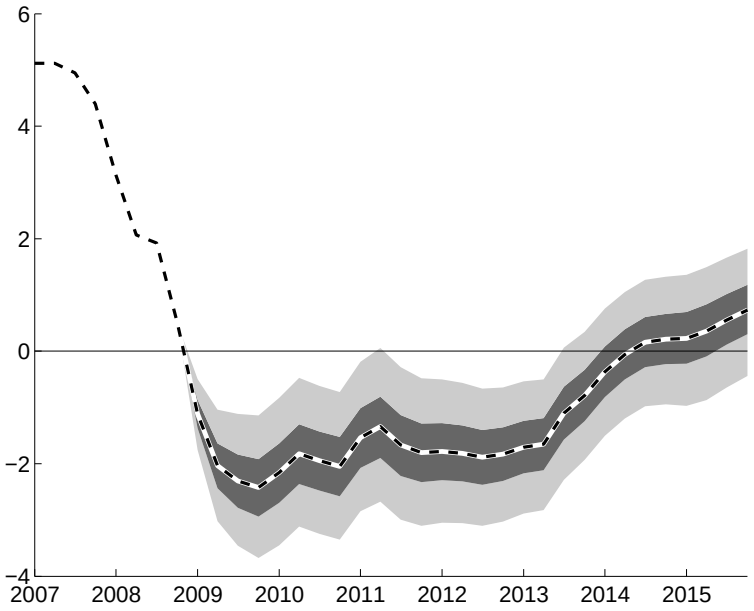

(b) Treating ELB Data as Missing

Note: Shaded areas indicate 50 and 90 percent uncertainty bands, dashed lines are posterior means. The posterior distribution is derived from conditioning the model on the entire data sample 1960:Q1 – 2015:Q4. Uncertainty bands reflect the joint uncertainty about model parameters and states. Results in Panel (b) are conditioned on a data set where observations on short–term rates are treated as missing data during the ELB period.

Figure 3: Shadow Rate Estimates, A Comparison

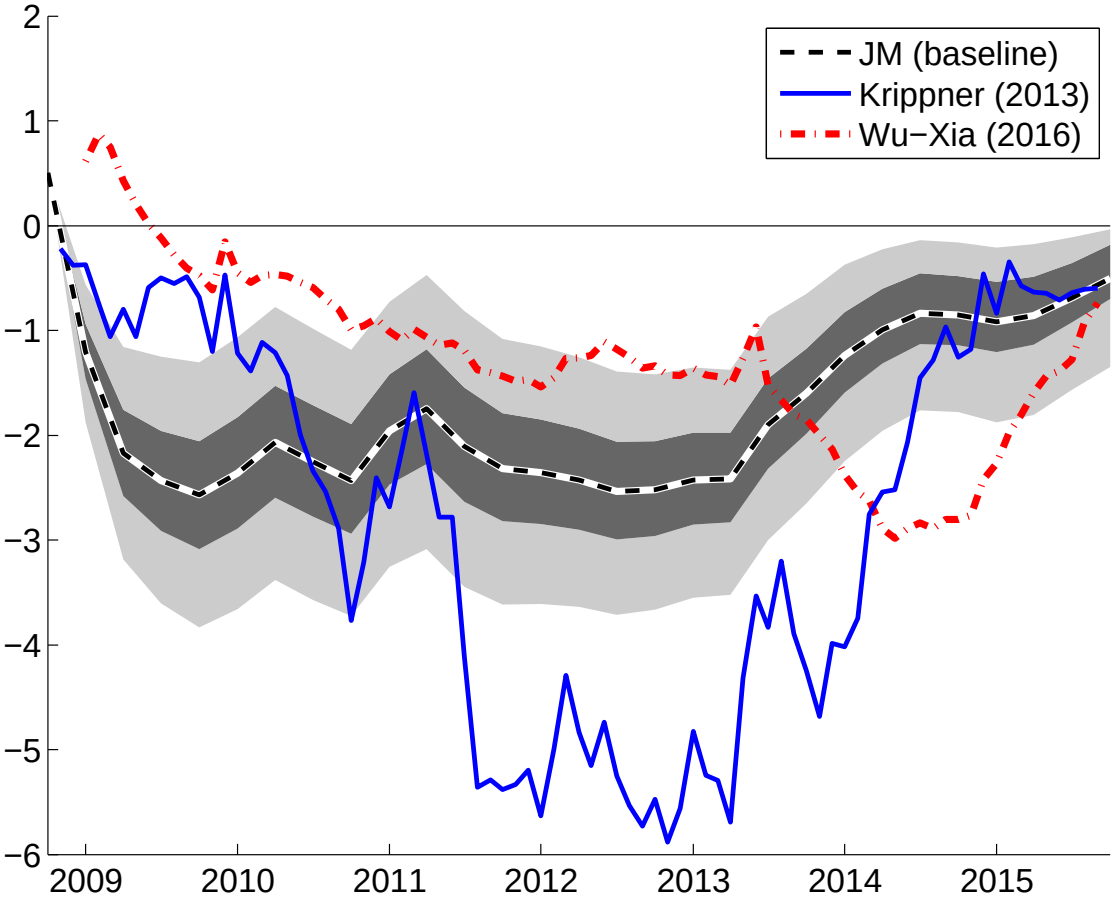

Note: Shaded areas indicate 50 and 90 percent credible sets, dashed lines are posterior means from our baseline model ("JM baseline"). The posterior distribution is derived from conditioning the model on the entire data sample 1960:Q1 – 2015:Q4. Uncertainty bands reflect the joint uncertainty about model parameters and states.

Figure 4: The Real Rate in the Long Run

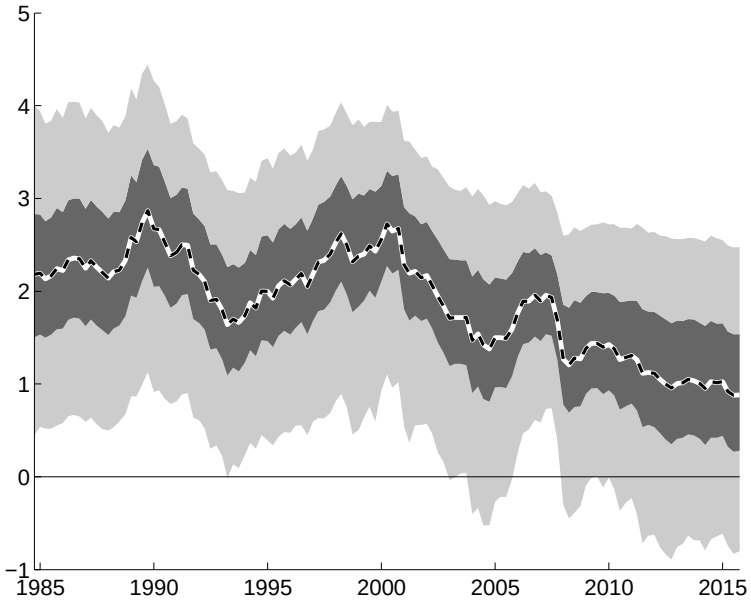

(a) Quasi Real–Time Estimate

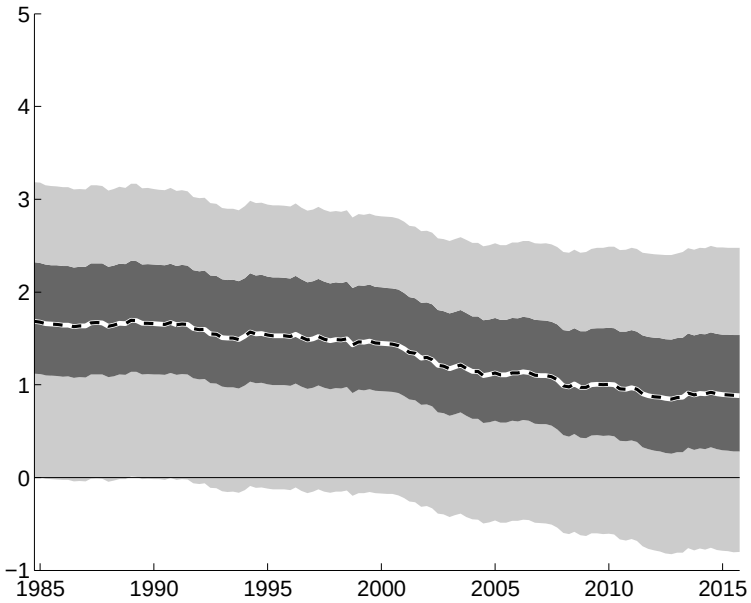

(b) Smoothed Estimates

Note: Shaded areas indicate 50 and 90 percent uncertainty bands, dashed lines are posterior means. Results shown in Panel (a) reflect the endpoints of sequentially re-estimating the entire model over growing samples of quarterly observations starting in 1960:Q1, thus reflecting "filtered" estimates of the model's latent variables. Results shown in Panel (b) reflect "smoothed" estimates using all available observations from 1960:Q1 through 2015:Q4. Uncertainty bands reflect the joint uncertainty about model parameters and states.

Figure 5: The Trend Nominal Rate when the ELB is Ignored

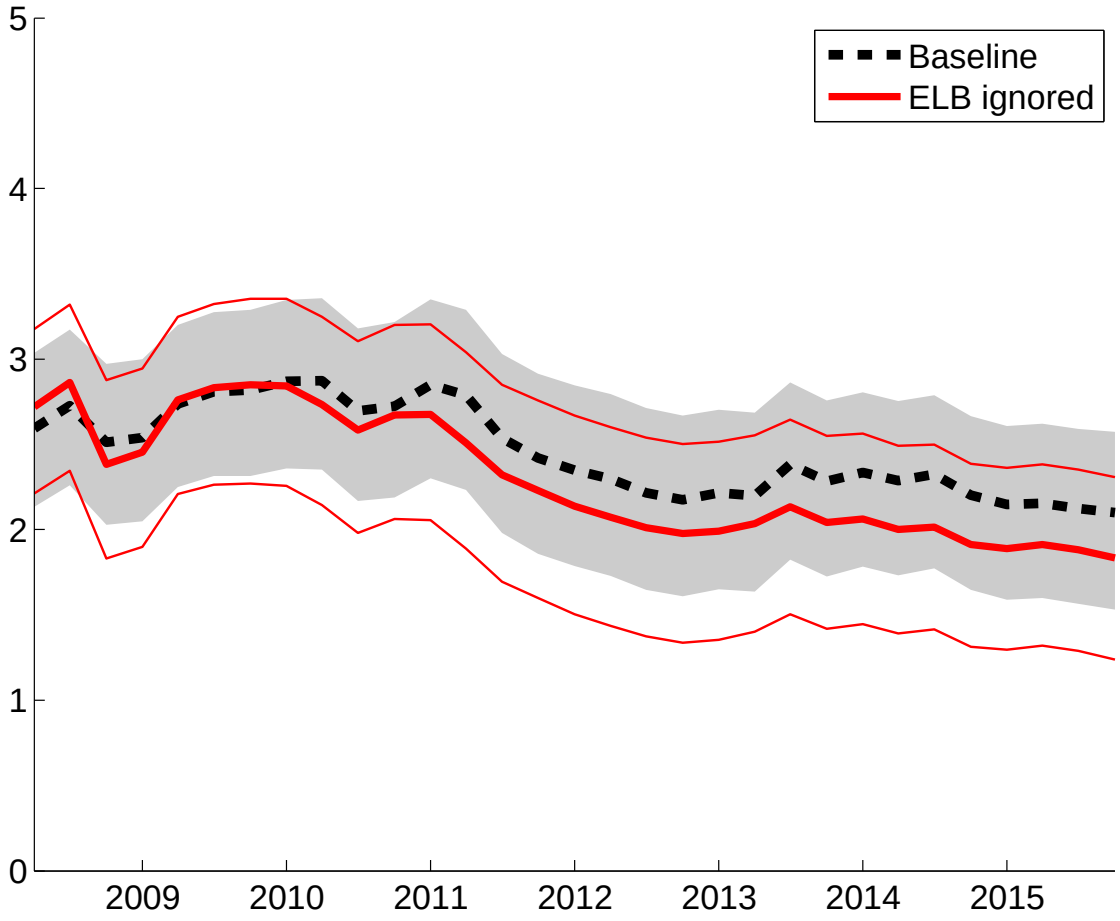

Note: Shaded area indicates 50 percent uncertainty bands and the dashed line is the mean estimate for our baseline model. This solid red lines indicate 50 percent uncertainty bands and the thick solid red line is the mean estimate when we ignore the ELB. The posterior distribution is derived from conditioning the model on the entire data sample 1960:Q1 – 2015:Q4. Uncertainty bands reflect the joint uncertainty about model parameters and states.

Figure 6: Estimates With and Without Medium–Term Yield

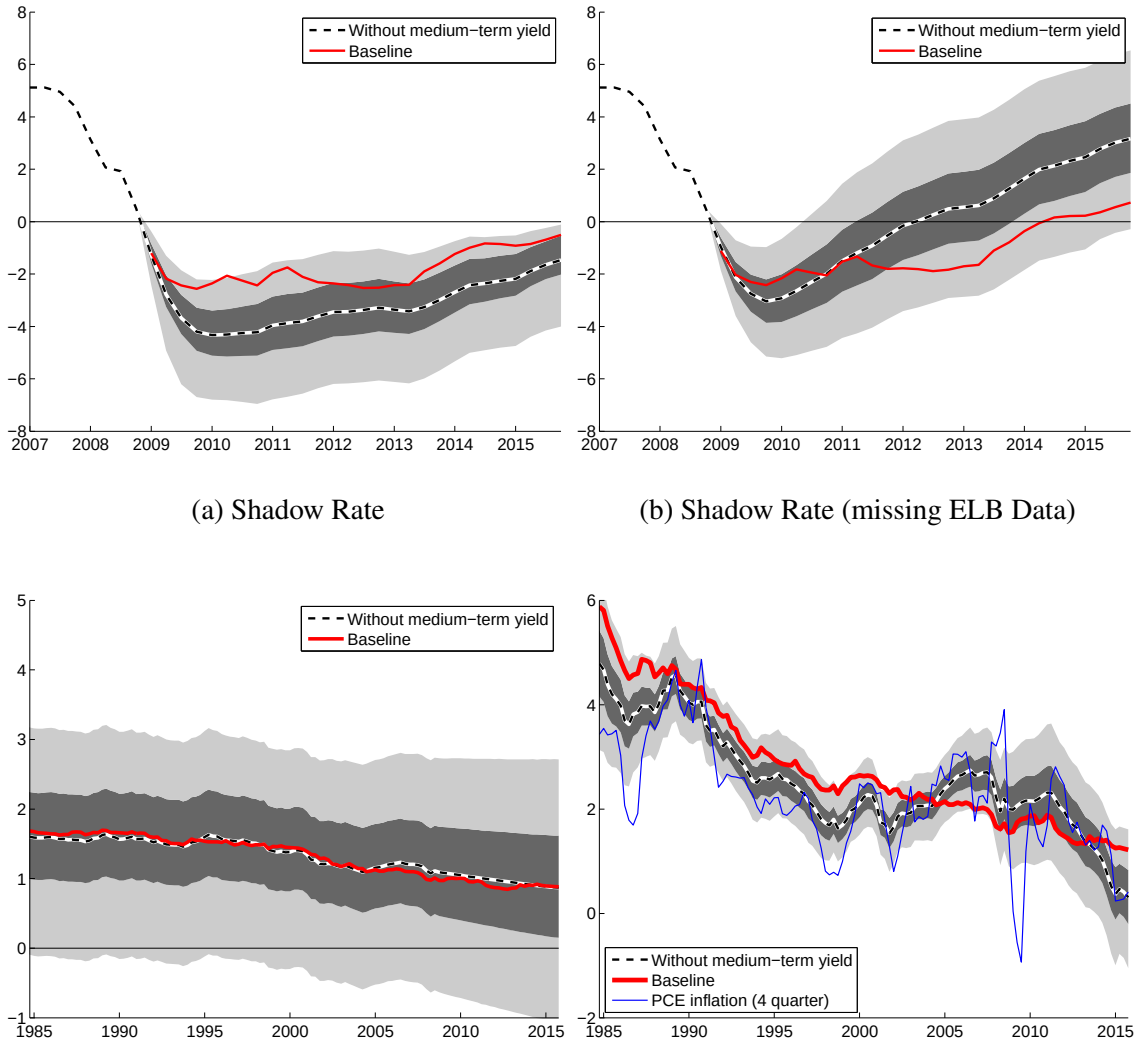

(a) Shadow Rate

(b) Shadow Rate (missing ELB Data)

(c) Real Rate Trend

(d) Inflation Trend

Note: Shaded areas indicate 50 and 90 percent credible sets, dashed and solid lines are posterior means derived from the smoothed, full-sample posterior of the respective models. The posterior distribution is derived from conditioning the model on the entire data sample 1960:Q1 – 2015:Q4. Uncertainty bands reflect the joint uncertainty about model parameters and states. Results in Panel (b) are conditioned on data sets where observations on short–term rates are treated as missing data during the ELB period.

Figure 7: Short–Term Interest Rate Forecasts, Start of ELB

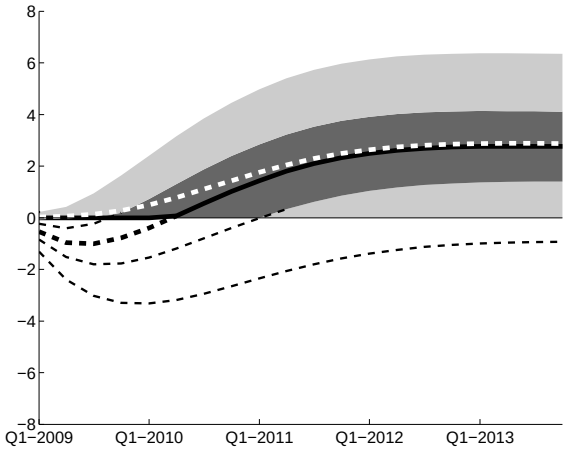

(a) Forecasts from 2008:Q4, Baseline

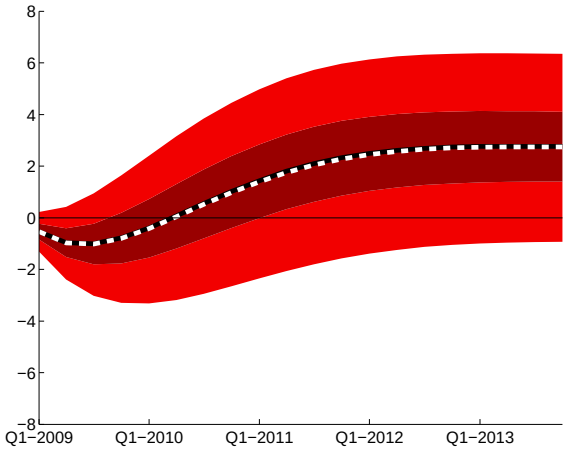

(b) Forecasts from 2008:Q4, Ignoring ELB

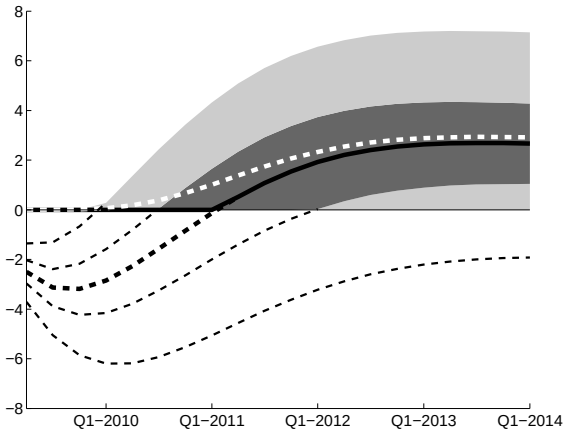

(c) Forecasts from 2009:Q1, Baseline

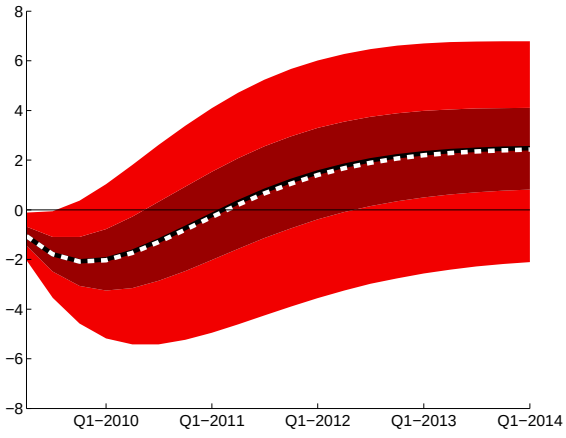

(d) Forecasts from 2009:Q1, Ignoring ELB

Note: Shaded areas indicate 50 and 90 percent credible sets, solid lines are posterior medians, wide dashed lines are posterior means of the projected interest rate. In the left panels, dashed lines less than the ELB are the posterior median and 50 and 90 percent credible sets of the shadow rate.

Figure 8: Short–Term Interest Rate Forecasts, During ELB

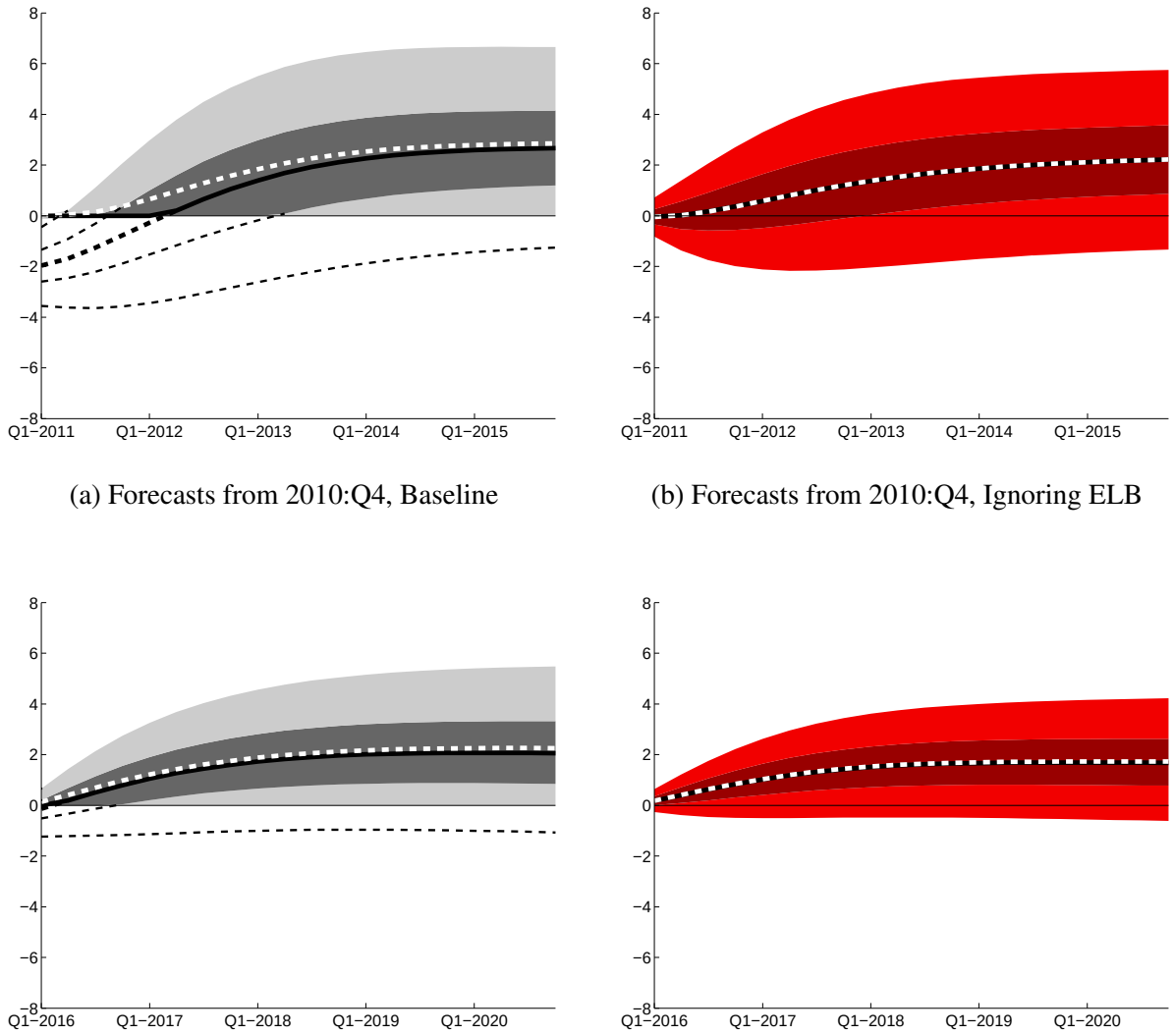

(a) Forecasts from 2010:Q4, Baseline

(b) Forecasts from 2010:Q4, Ignoring ELB

(c) Forecasts from 2015:Q4, Baseline

(d) Forecasts from 2015:Q4, Ignoring ELB

Note: Shaded areas indicate 50 and 90 percent credible sets, solid lines are posterior medians, wide dashed lines are posterior means of the projected interest rate. In the left panels, dashed lines less than the ELB are the posterior median and 50 and 90 percent credible sets of the shadow rate.

Figure 9: Time-varying Uncertainty about Future Short–Term Interest Rates

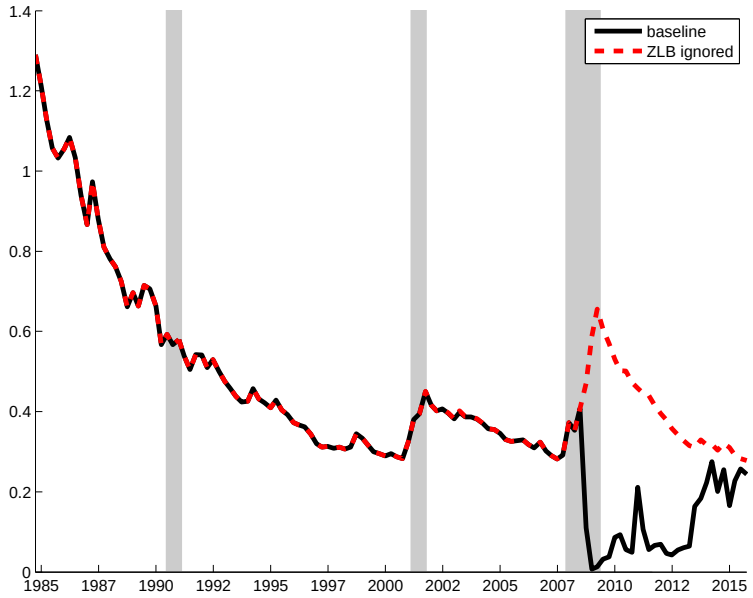

(a) One-quarter ahead uncertainty

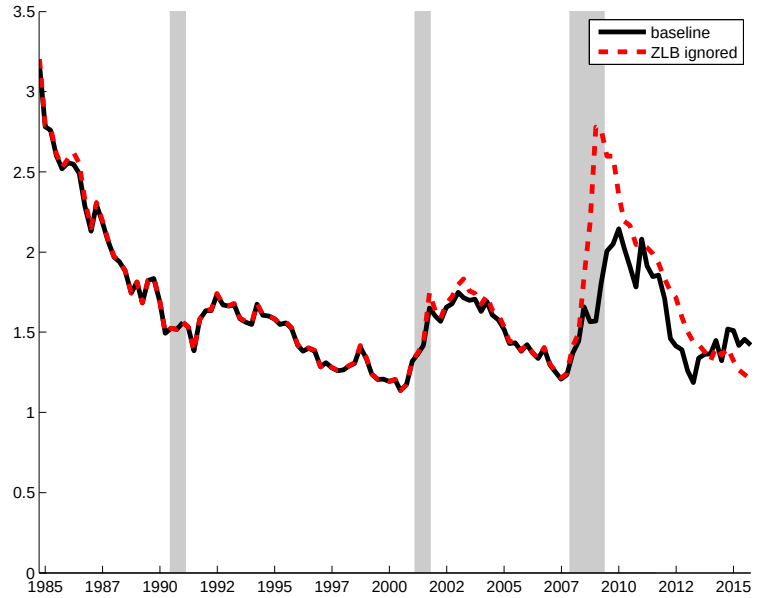

(b) Eight-quarter ahead uncertainty

Note: Forecast uncertainty about future short–term interest rates as measured by the standard deviation of each model's predictive densities for i_t. The predictive densities are re-estimated over growing samples that all start in 1960:Q1. In the baseline model (black solid lines), the predictive density is truncated at the ELB, whereas no constraint is imposed on the predictive density in the alternative model that ignores the ELB (red dashed line).

Figure 10: Expectations Component of the 5-year Rate

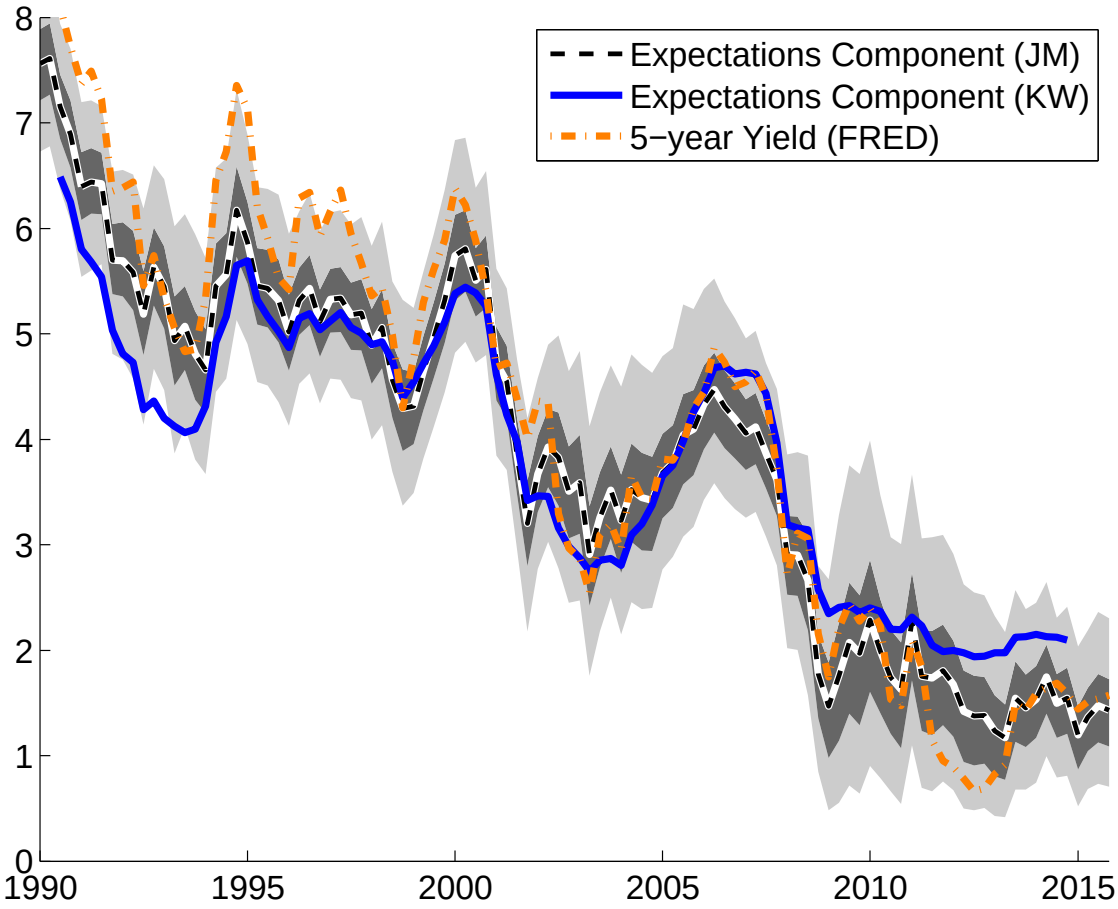

Note: Shaded areas indicate 50 and 90 percent credible sets and wide dashed lines are posterior means of the estimated 5–year term–premium in our model. The red solid line is the estimated 5–year term–premium when we ignore the ELB.

Table 1: Forecast Evaluation (Through 2007)

	Forecast horizon h				
	1	2	3	4	8
Panel A: Short-term interest rate i_{t+h}					
	baseline				
RMSE	0.33	0.69	1.02	1.34	2.20
MAD	0.25	0.53	0.81	1.08	1.78
PS	0.58	−0.69	−1.37	−1.86	−2.81
	ELB ignored				
rel. RMSE	1.00	1.00	1.00	1.00	1.00
rel. MAD	1.00	1.00	1.00	1.00	1.00
rel. PS	-0.99^{***}	-0.44^{***}	-0.15^{**}	0.02	0.33^{***}
	without medium-term yield				
rel. RMSE	1.12^{**}	1.06	1.02	1.00	0.98
rel. MAD	1.11^{*}	1.04	1.00	0.97	0.98
rel. PS	-0.15^{***}	0.01	0.05	0.07	0.06
Panel B: Long-term interest rate y_{t+h}					
	baseline				
RMSE	0.45	0.73	0.91	1.09	1.40
MAD	0.37	0.61	0.74	0.89	1.10
PS	0.22	−0.65	−1.06	−1.37	−1.92
	ELB ignored				
rel. RMSE	1.00	1.00	1.00	1.00	1.00
rel. MAD	1.00	1.00	1.00	1.00	1.00
rel. PS	-0.89^{***}	-0.49^{***}	-0.31^{***}	-0.20^{***}	0.02

Note: *RMSE* are root-mean-squared errors computed from using each the means of each model's predictive densities as forecasts; *MAD* are mean absolute deviations obtained from using the medians of each model's predictive densities. *PS* are average predictive scores. Relative RMSE and MAD are expressed as ratios relative to the corresponding statistics from the baseline model (values below unity denoting better performance than baseline); predictive scores are expressed as differences relative to the baseline (positive values denoting better performance than baseline). Predictive densities are re-estimated over growing samples that all start in 1960:Q1. For the forecast evaluation, the first forecast jumps off in 1984:Q4 and the last in 2007:Q4. Stars indicate significant differences, relative to baseline, in squared losses, absolute losses and density scores, respectively, as assessed by the test of Diebold and Mariano (1995); ***, ** and * denote significance at the 1%, 5% respectively 10% level.

Table 2: Forecast Evaluation (Post 2007)

	Forecast horizon h				
	1	2	3	4	8
Panel A: Short-term interest rate i_{t+h}					
	baseline				
RMSE	0.21	0.36	0.61	0.84	1.82
MAD	0.05	0.11	0.23	0.36	1.27
PS	−0.13	−0.41	−0.68	−0.88	−1.43
	ELB ignored				
rel. RMSE	1.64	1.63^{*}	1.35^{*}	1.18^{**}	0.88^{**}
rel. MAD	4.41^{***}	3.99^{***}	2.78^{***}	2.37^{***}	1.16
rel. PS	−0.13	-0.47^{***}	-0.58^{***}	-0.62^{***}	-0.55^{***}
	without medium-term yield				
rel. RMSE	1.21	1.08	1.09	1.07	1.05
rel. MAD	1.33	0.98	0.79	0.78	1.03
rel. PS	−0.06	0.01	0.04	0.07	0.09
Panel B: Long-term interest rate y_{t+h}					
	baseline				
RMSE	0.36	0.63	0.78	0.90	1.52
MAD	0.28	0.46	0.62	0.76	1.24
PS	0.61	−0.33	−0.76	−1.03	−1.90
	ELB ignored				
rel. RMSE	1.05^{**}	1.05	1.05	1.05	0.97
rel. MAD	1.06^{*}	1.03	1.04	1.02	0.96
rel. PS	-1.00^{***}	-0.59^{***}	-0.40^{***}	-0.28^{***}	0.10

Note: *RMSE* are root-mean-squared errors computed from using each the means of each model's predictive densities as forecasts; *MAD* are mean absolute deviations obtained from using the medians of each model's predictive densities. *PS* are average predictive scores. Relative RMSE and MAD are expressed as ratios relative to the corresponding statistics from the baseline model (values below unity denoting better performance than baseline); predictive scores are expressed as differences relative to the baseline (positive values denoting better performance than baseline). Predictive densities are re-estimated over growing samples that all start in 1960:Q1. For the forecast evaluation, the first forecast jumps off in 2008:Q1 and the last in 2015:Q4. Stars indicate significant differences, relative to baseline, in squared losses, absolute losses and density scores, respectively, as assessed by the test of Diebold and Mariano (1995); ***, ** and * denote significance at the 1%, 5% respectively 10% level.